Coordination Chemistry Reviews 254 (2010) 954–971

Contents lists available at ScienceDirect

Coordination Chemistry Reviews

journal homepage: www.elsevier.com/locate/ccr

Review

Recent advances in arylene ethynylene folding systems: Toward functioning

Ben-Bo Ni, Qifan Yan, Yuguo Ma*, Dahui Zhao*

Beijing National Laboratory for Molecular Sciences (BNLMS), Key Laboratory of Polymer Chemistry and Physics of Ministry of Education, College of Chemistry and Molecular Engineering, Peking University, Beijing 100871, China

Contents

ARTICLE INFO

Article history:
Received 30 November 2009
Accepted 4 February 2010
Available online 11 February 2010

Keywords:
Foldamers
Arylene ethynylene
Supramolecular chemistry
Guest binding
Aromatic stacking
Solvophobic interaction

ABSTRACT

Well-defined 3-dimensional architectures constitute the indispensable structural basis of the versatile, mind-boggling functions of biological macromolecules, such as proteins and nucleic acids. In the past few decades, diversified synthetic systems have been designed to mimic these biological entities in their capability of adopting such specific, higher order structures. The relevant research field presents one of the most rapidly developing areas related to supramolecular chemistry. The current contribution will focus on the most recent progress related to foldamers consisting of arylene ethynylene building blocks. Some of the work features developing novel functions based on previously established arylene ethynylene folding systems, and others have designed and synthesized new arylene ethynylene foldable structures that aim to realize previously uncharted properties.

1. Introduction and scope

Well-defined 3-dimensional architectures constitute the indispensable structural basis of the versatile, mind-boggling functions of biological macromolecules (e.g., proteins, nucleic acids). In the past few decades, diversified synthetic systems have been designed to mimic these biological entities in their capability of adopting such specific, higher order structures. The relevant research field presents one of the most rapidly developing areas related to supramolecular chemistry [1–25]. The word "foldamer" was specifically coined to refer to "any oligomer that folds into a conformationally ordered state in solution, the structures of which are stabilized by a collection of noncovalent interactions between non-adjacent monomer units", or more broadly, "any polymer

* Corresponding authors.
E-mail addresses: ygma@pku.edu.cn (Y. Ma), dhzhao@pku.edu.cn (D. Zhao).

0010-8545/$ – see front matter © 2010 Elsevier B.V. All rights reserved.
doi:10.1016/j.ccr.2010.02.004

with a strong tendency to adopt a specific, compact conformation" [4]. With new foldable structures being continuously designed and synthesized, more and more efforts are consciously made at modulating and controlling the folding behaviors through identifying correlation between folded conformations and chemical structures. More importantly, developing foldable systems that are capable of performing certain functions has become an emerging but marked focus of the researchers, either by further decorating the previously developed foldamer scaffolds, or by designing novel structures.

Among the various synthetic molecules of the foldamer family, oligo- and poly(arylene ethynylene)s represent an important group. Ever since the folding behaviors of *m*-phenylene ethynylene (*m*PE) oligomers were first reported by Moore and coworkers in 1997 [26], *m*PE and related arylene ethynylene foldamer systems have been extensively developed and investigated [27–39]. Compared with many other foldamer systems containing non-natural, aromatic units, such as aromatic oligoamides [15,16,40–43], arylene polymer/oligomers [21,24,25,44–55], poly(phenylacetylene)s [21,23,56–58], *iso*-polydiacetylenes [59,60], poly(*N*-propargylamides) [61], poly(*N*-octylcarbazole ethylene) [62], polydiacetylene [63], etc., arylene ethynylene foldable systems (AEFS) exhibit a distinct feature that they mainly rely on weak, noncovalent interactions among non-adjacent backbone units to realize folding. Those noncovalent forces that typically exist among neighboring repeat units and are often harnessed to realize folding in alternative foldamer systems, such as steric, torsional, and hydrogen bonding interactions, are usually absent in AEFS. The devoid of steric and torsional interactions in AEFS is due to the periodic insertion of the ethynylene segment in the backbone. One of the reasons for noncovalent interactions among non-adjacent subunits to be of particular interest and worthy of scrutiny is that such interactions are ubiquitous and crucial in the supramolecular structures of biomacromolecules, e.g., in protein folding. In this regard, another large group of foldamers, i.e., peptoid series, share the unique characteristic with AEFS of exploiting interactions between non-adjacent backbone units to achieve folding. Yet, peptoid foldamers commonly depend on hydrogen bonding interactions, while designing and developing AEFS usually deal with weak, non-directional forces such as aromatic stacking and/or solvophobic interactions.

In addition to their unique structures and folding capabilities, AEFS are of particular research interest for following reasons. Firstly, as mentioned above the aromatic scaffolds typically rely on π–π stacking among non-adjacent repeat units and/or backbone solvophobic effects to stabilize the folded conformation. As these forces are weak noncovalent interactions, the resultant folded structures are usually dynamic and flexible. Such structural flexibility can accommodate conformational adjustments and adaptations in response to external stimuli and/or interactions with other molecules (e.g., binding). This is in contrast to particularly rigid folded architecture. Secondly, modularly constructed AEFS allow for facile chemical modifications, facilitating convenient tailoring of the folding properties as well as function designs. Additionally, under the folded conformations AEFS typically possess a defined inner cavity, which provides a special opportunity for developing functional bio-system mimicry (e.g., artificial enzymes).

Since there are previously published reviews and book chapters that have comprehensively summarized earlier work on foldamers or have highlighted specific relevant topics [4,9,10,64–68], the current contribution will only focus on the most recent progress related to foldamers consisting of arylene ethynylene building blocks [69–80]. Some of the work features developing novel functions based on previously established AEFS, and others have designed and synthesized new AEF structures that aim to realize previously uncharted properties. Also, by introducing representative examples we attempt to illustrate some general trend of the research in this area.

2. Function-oriented design and development of novel AEFS

2.1. Guest binding

Host–guest binding events involving various types of noncovalent interactions represent an important topic of supramolecular chemistry. Its significance in part originates from its analogy with substrate binding of proteins. Using synthetic systems to achieve guest binding with selectivity, or even specificity, undoubtedly denotes a key step down the road of realizing enzyme mimicry. For AEFS, various structures capable of binding neutral molecules, cations, or anions have been reported.

2.1.1. Small-molecule guest binding of mPE foldamers

The seminal work on *m*PE oligomers binding terpene molecules was first reported in 2000 by Moore and coworkers [64]. The driving force for this binding event was proposed to mainly originate from the solvophobic effect. By extending the length of the side chains from tri(ethylene glycol) to hexa(ethylene glycol), *m*PE dodecamer **1b** (Fig. 1) became soluble in water, where the driving force of solvophobicity could be maximized [81]. Folding study on the dodecamer **1b** was performed in CH_3CN/H_2O binary solvents by monitoring the UV–vis absorption and the binding of (−)-α-pinene in the same solvent series was investigated using CD spectroscopy. The CD signal remained silent until the volume percentage of water reached over 50%. The strongest binding was observed in solution containing 90% water, under which conditions the host–guest ratio was determined to be 1:1 with a binding constant of $1.4 \times 10^6\ M^{-1}$. In comparison, for dodecamer **1a**, induced Cotton effect was previously observed to emerge at water percentage as low as 10% [64]. The author speculated that the longer side chain was able to insert into the helical cavity, inhibiting guest binding at lower compositions of water. Kinetic studies on the binding process also revealed solvent composition-dependent behaviors. Namely, significantly slower binding kinetics was observed with solutions of a high water composition. On the basis of these results, a tighter folding was suggested under such conditions.

In an independent study, a short amide sequence was incorporated in the middle of the *m*PE oligomers (Fig. 2) [82]. Such structural modifications did not significantly affect the folding stability of the chain, as indicated by the UV–vis absorption change upon varying the ratio of $CHCl_3$ and CH_3CN in a solvent titration experiment.

None of the three oligomers **2**–**4** containing varied amide sequences showed detectable affinity to the neutral form of the rod like amine **5** in CH_3CN, indicated by the CD signal silence in the *m*PE absorption region. However, after HCl was added in the solution, *m*PE **2** (and only *m*PE **2**) displayed an induced CD signal, indicative of its complexation with **5**. The binding affinity of the

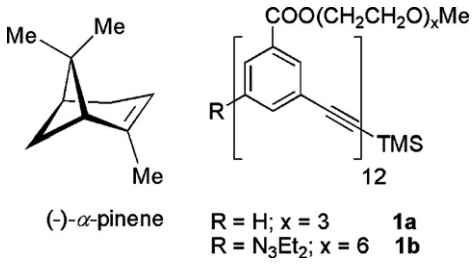

Fig. 1. Chemical structures of (−)-α-pinene and oligo(ethylene glycol) appended *m*PE dodecamers **1a** and **1b** [81].

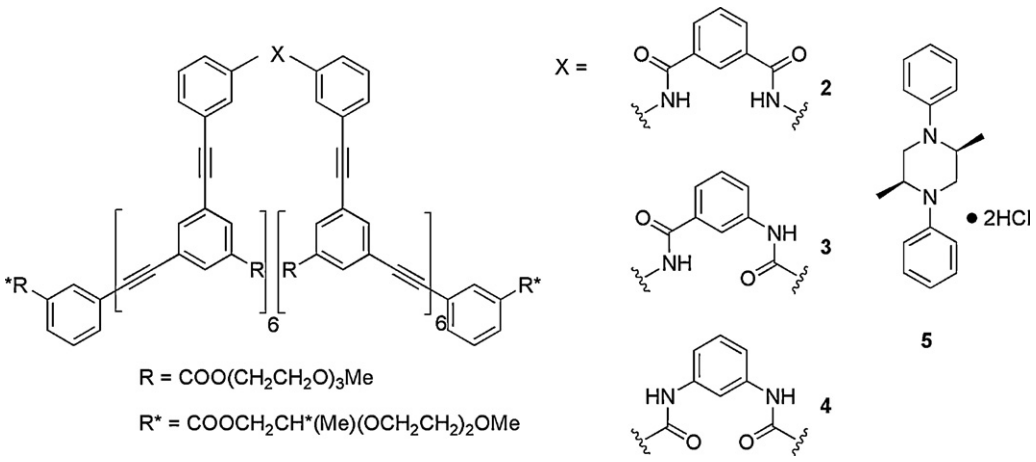

Fig. 2. Chemical structures of *m*PE foldamers **2**–**4** incorporating varied amide sequences and piperazinium dihydrochloride salt **5** [82].

oligomer for the guest molecule was proposed to originate from specific hydrogen bonding interactions. This was supported by an NMR study showing the chemical shift change of the amide N*H* in a model compound upon mixing with piperazinium dihydrochloride salt **5**. The sequence selectivity was hypothesized to be related to different amide group orientations in the folded conformation of varied oligomers.

2.1.2. Poly- and oligo(meta-ethynylpyridine)s as helical hosts for saccharides

Using poly- and oligo(*m*-ethynylpyridine)s as the scaffold, Inouye et al. carried out systematic studies on their folding properties upon binding with saccharide molecules [36]. Although molecules **6** and **7** exhibited certain intramolecular π–π interactions, as evidenced by partial quenching of the major emission band accompanied by the emergence of a new excimer-like emission at longer wavelengths, these sequences were believed to mainly exist in disordered conformations in chlorinated hydrocarbon solvents. The preference for the non-folded conformations was partly attributed to the dipole–dipole interaction between neighboring pyridine units, i.e., adjacent dipole moments preferred to be oriented in an anti-parallel fashion.

However, when *n*-octyl-β-glucopyranoside **8** was added to a solution of **6** or **7** in CH_2Cl_2, a decrease in the extinction coefficient of the chain molecule was observed, and an induced CD signal was also detected. These results indicated that the saccharide derivative was binding to the *m*-ethynylpyridine oligomer/polymer, and its chirality had influenced the handedness bias of the folded chain. Control experiments showed no evidence for the polymer/oligomer binding with methyl substituted saccharides. It was thus suggested that the affinity of saccharide **8** for the *m*-ethynylpyridine oligomer/polymer most likely resulted from hydrogen bonding interactions.

The observation that in the presence of the saccharide the CD signal only emerged from *m*-ethynylpyridine oligomers of longer chain lengths but remained silent for shorter oligomers confirmed the postulation about the binding-induced helical conformation of the oligomers (Fig. 3). A 1:1 binding stoichiometry and an association constant of $1.2 \times 10^3\ M^{-1}$ were determined for the complex formed by **7** and **8**. The high affinity of *m*-ethynylpyridine oligomers for saccharide molecules even allowed extraction of native saccharides into less polar organic solvents, such as CH_2Cl_2 and $CHCl_3$.

By replacing the alkoxypyridyl units with dialkylaminopyridyl in the aforementioned polymer, a basic poly(*m*-ethynylpyridine) **9** was obtained [83]. Subsequent UV–vis absorption studies indicated a quantitative binding of the pyridine units in polymer **9** with protons from trifluoroacetic acid (TFA) (Fig. 4).

Similar to polymer **6**, the basic polymer **9** binds with saccharides, evidenced by the occurrence of induced CD signals. Moreover, protonation of the pyridine rings in the polymer chain brought about an interesting effect on the stability of the polymer–saccharide binding complex. The highest ellipticity was attained after the first 0.5 equiv. (relative to the number of the pyridine units) of TFA

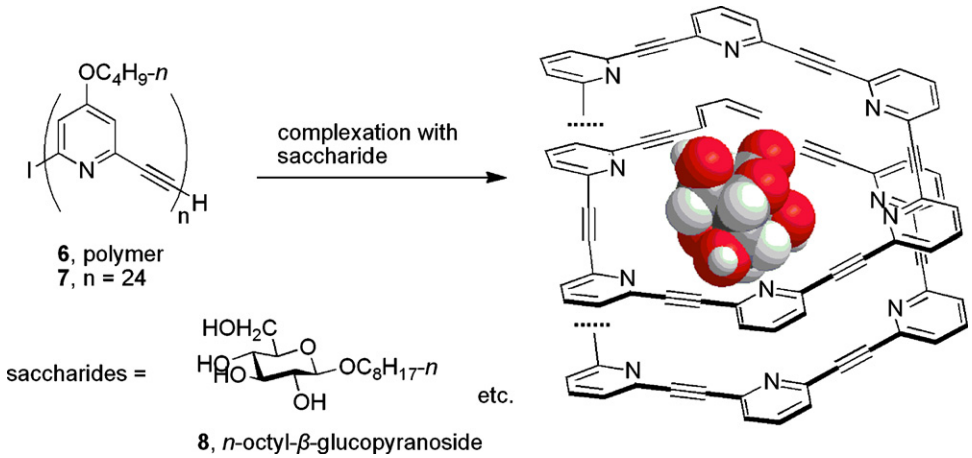

Fig. 3. Schematic representation showing the binding of poly- and oligo(*m*-ethynylpyridine)s **6** and **7** with saccharides **8** [36]. (Side chains were omitted in the folded conformation for clarity, reproduced with permission from Ref. [36].)

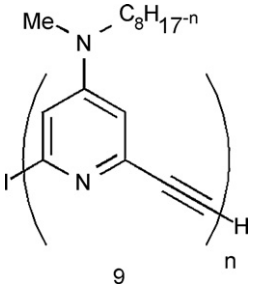

Fig. 4. Structure of basic poly(*m*-ethynylpyridine) **9** [83].

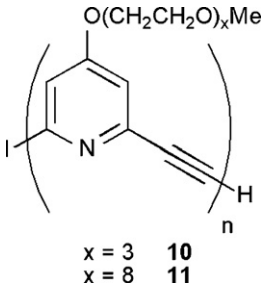

Fig. 6. Structures of polymers **10** and **11** [84].

was added, but further addition of TFA suppressed the induced CD signals. This result indicated that half protonated form of the polymer exhibited the highest affinity to the guest hexoses. On the basis of quantitative analyses, upon addition of 0.5 equiv. of TFA, formal binding constants between the polymer and various saccharide molecules increased by a factor of 2–200, depending on the structure of the saccharides.

The reason for this enhancement in saccharide binding affinity observed for the poly(*m*-ethynylpyridine) upon protonation was considered to be a result of alternating dipoles in the half-protoned backbone. As shown in Fig. 5, when every other pyridine unit is protoned, the alternatively oriented local dipole moments in the backbone would prefer an all-cisoid chain conformation, which is more favorable for folding as well as for binding the saccharide molecule. Additionally, it was proposed that the pyridinium–pyridine stacking interaction between neighboring turns in the helix may further stabilize the folded conformation and thus favor guest binding. This speculation was supported by DFT calculations.

With oligo(ethylene glycol) side chains appended at 4-position of the pyridine rings, poly(*m*-ethynylpyridine) was made soluble in polar solvents and capable of binding native saccharides [84]. Specifically, polymer **10** was soluble in MeOH/H_2O (10/1), and polymer **11** with even longer ethylene glycol side chains was soluble in pure water. Binding between **11** and native saccharides in water was monitored by CD spectroscopy (Fig. 6).

Mutarotation is a special feature of native glucoses, taking place via a reversible hemiacetal formation. Interestingly, the mutarotation process influences the handedness of the host helices (Fig. 7). When pure α-D-glucose was bound to poly(*m*-ethynylpyridine) **11** in MeOH/H_2O through hydrogen bonding, a negative CD signal of −3 mdeg was observed initially. However, after 48 h the CD signal gradually changed and turned to +2.4 mdeg. In contrast, complex formed by pure β-D-glucose and polymer **11** initially gave a CD signal of +7 mdeg, but the magnitude of the signal gradually decreased to +2.4 mdeg after 48 h. Moreover, while the CD spectra were changing over time, the UV–vis absorptions were monitored simultaneously and showed hardly any change. It was thus suggested that the origin of the altered CD signals was the helix inversion of the host polymer (Fig. 7), rather than partial dissociation of the complex [85]. It was then postulated that the different stereochemical configurations of C1 in glucoses, α and β, led poly(*m*-ethynylpyridine) to adopt helical conformations of opposite handedness, which was illustrated by opposite signs and different magnitudes (i.e., −3 and +7 mdeg, respectively) of the initial CD signals. As the mutarotation proceeded with

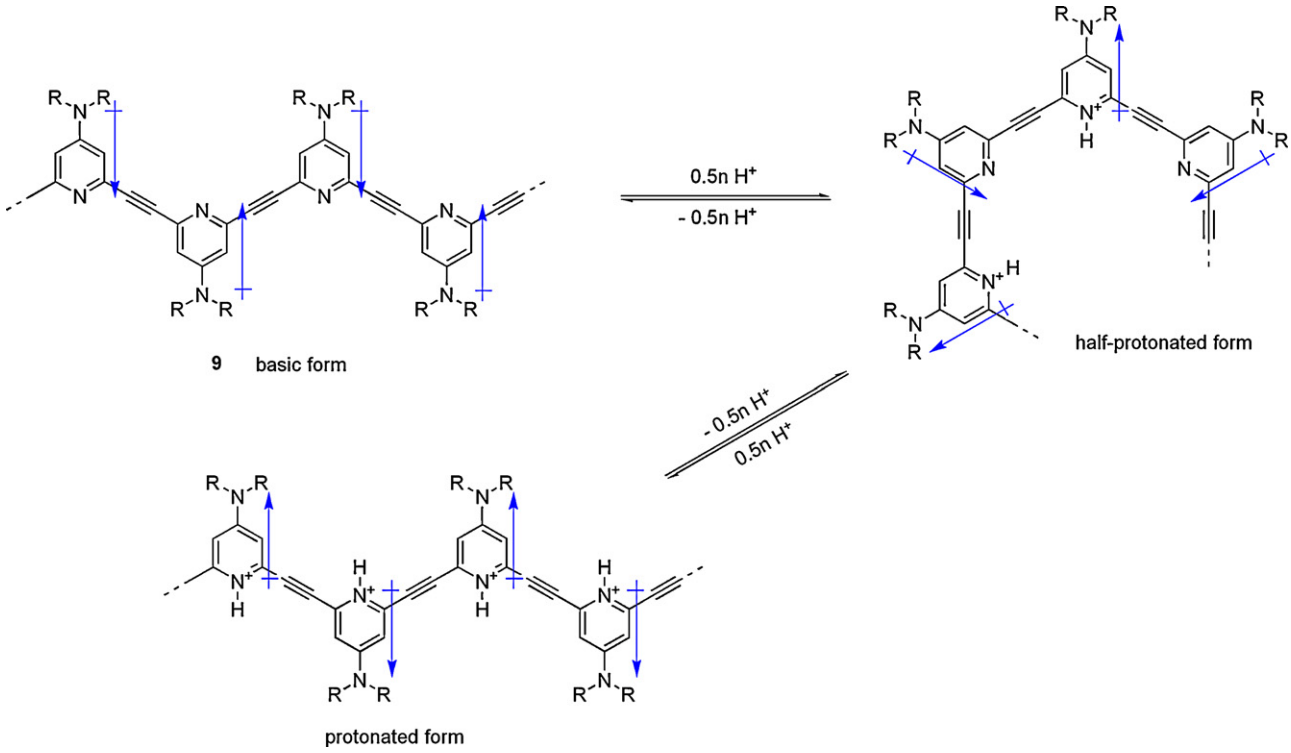

Fig. 5. Schematic illustration of the influence of protonation over the local conformation of polymer **9** [83].

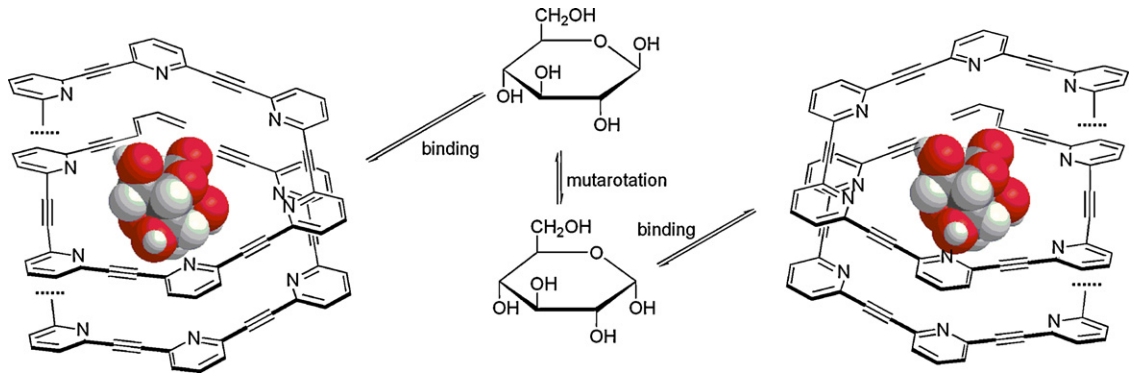

Fig. 7. Illustration of mutarotation induced helicity inversion of **11** [85].

the saccharide, the chirality of the helices changed accordingly between *M* and *P* states, until the mutarotation reached the equilibrium.

The thermodynamic free energy change of the saccharides binding to the polymer should involve both enthalpy gain and entropy loss. The former may result from secondary interactions, e.g., hydrogen bonding between the host and guest as well as intramolecular π–π stacking of the polymer. While the latter was due to the transition from disordered states to the more ordered helical conformation by the polymer, in addition to the loss of a free guest molecule [86]. Covalent linking a saccharide to one end of an oligo(*m*-ethynylpyridine) [87] through a flexible alkyl chain strengthened the helix conformation. This was reasonably explained as follows. The ligated system entails less of an entropy loss compared to a polymer binding a free guest molecule.

Subsequently, oligo(*m*-pyridineethynylene-*alt*-*m*-pyridone-ethynylene) **12** was synthesized by replacing every other pyridine in the original structure with pyridone units [88]. This unique oligomer was speculated to self-dimerize into duplexes through inter-strand hydrogen bonds between pyridine and pyridone units. This postulation was confirmed by the vapor pressure osmometry (VPO) and ^{1}H NMR studies. The duplexes of the longer oligomers were able to unwind and dissociate into single helix upon recognition of saccharide molecules. This process was monitored by following the induced CD signals (Fig. 8).

Azacrown, a known host for ammonium cations, was introduced at the 4-position of every third pyridine rings in a poly(*m*-ethynylpyridine) chain [89]. This novel modification was designed to bring about the following consequences. In the helical conformation of the polymer, the azacrown moieties align to host polyammonium cations and form pseudopolyrotaxenes. Triethylene tetramine (TETA) protonated by TFA stabilizes the induced folding of polymer **13** in the presence of a glucopyranoside (Fig. 9). Quantitative analyses using CD spectroscopy via a titration experiment gave a formal binding constant of $1.0 \times 10^2\ M^{-1}$ for the azacrown-attached polymer and β-1-O-*n*-octyl-glucopyranoside. Upon addition of TETA, the binding constant increased to $8.0 \times 10^2\ M^{-1}$, and it was further raised to $1.5 \times 10^3\ M^{-1}$ upon further addition of TFA.

2.1.3. Cation binding of m-ethynylenepyridine oligomers

An earlier study on the *m*PE oligomers by Moore et al. showed that by decorating the phenylene units in the backbone with cyano groups, the oligomer became capable of binding metal ions in the folded conformation [90]. Such cation binding ability was subsequently realized with alternative AEFS. These new cation-affinitive

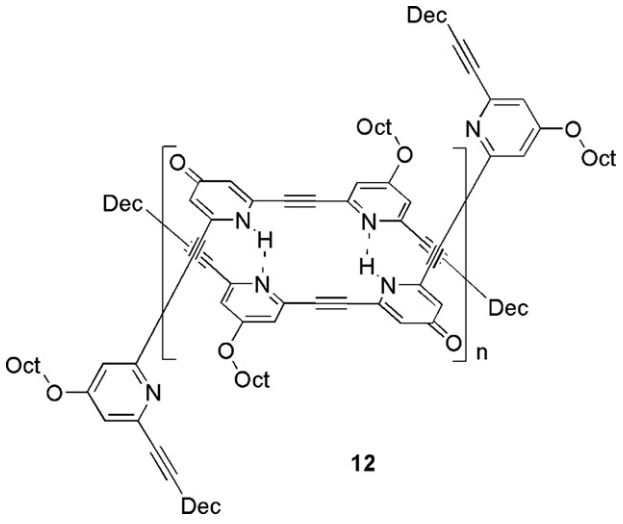

Fig. 8. Self-dimerized pyridine-pyridone oligomer **12** [88].

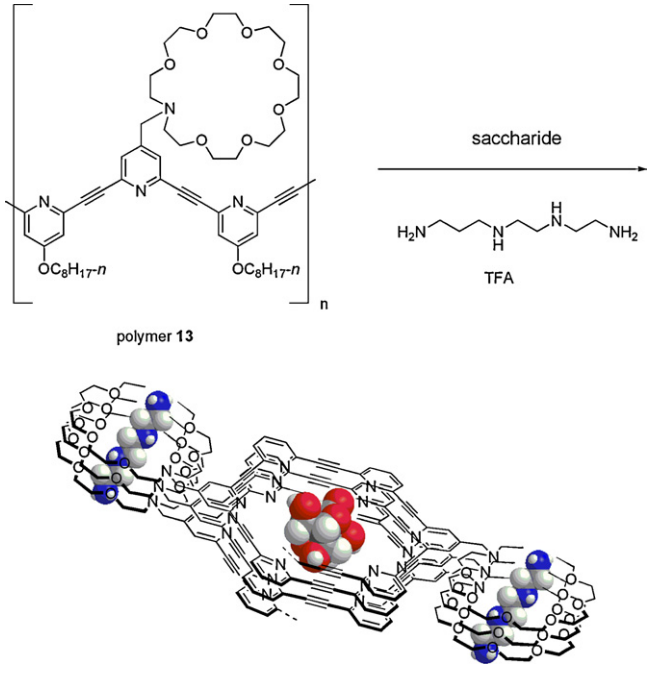

Fig. 9. Polyammonium cation assisted complexation of **13** with a saccharide [89]. (Spheres in blue: N atoms; red: O; grey: C; white: H.)

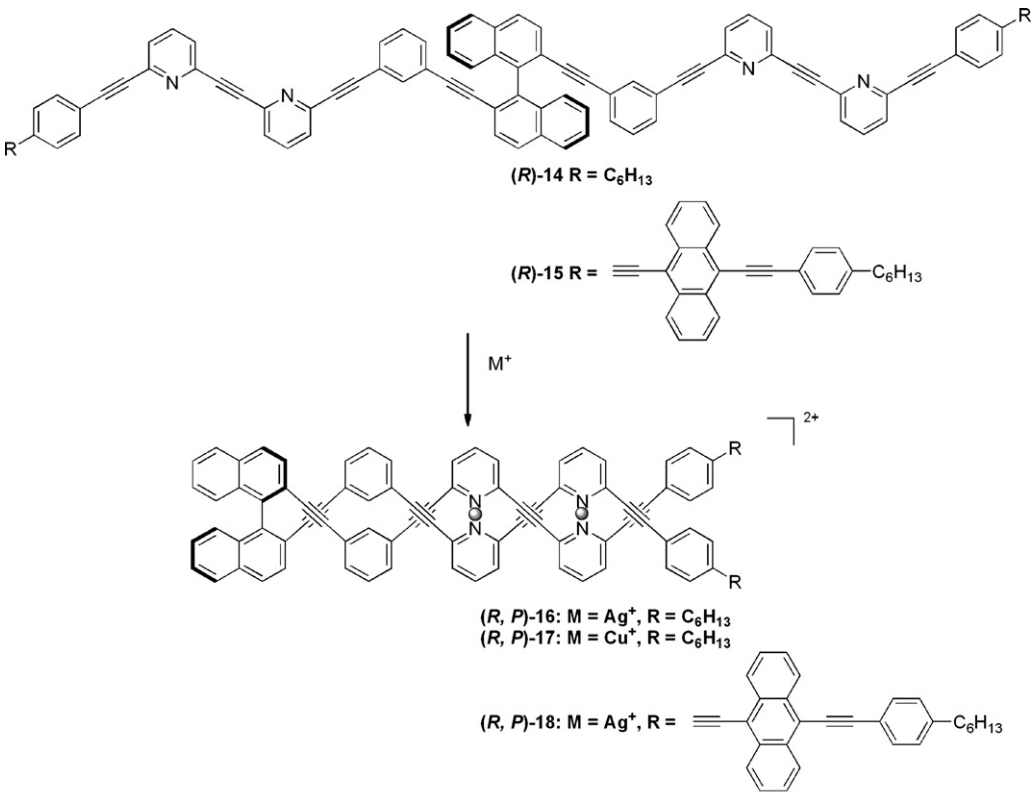

Fig. 10. Metal-assisted assembly of oligo(*m*-ethynylenepyridine)s (*R*)-**14** and (*R*)-**15** to double helicates (*R*, *P*)-**16**–**18** [91].

foldamers all include pyridine units as the coordinating moiety. Depending on the backbone structure, single-, double-, and triple-stranded helicates have all been observed.

Short oligo(*m*-ethynylenepyridine) sequences **14** formed double helicates **16** and **17** by coordinating to copper and silver ions [91,92], respectively. Chirality of the double stranded helicate of the silver complex **16** was confirmed by the emergency of a strong CD signal at 345 nm and a medium peak at 310 nm. Via a titration experiment monitored by CD spectroscopy, an association stoichiometry of 2:1 was determined for oligomer **14** binding with Cu^+ or Ag^+ [91]. Anthryl chromophores, having a long-wavelength absorption that does not overlap with the absorption of binaphthyl–arylacetylene moiety, were introduced into oligomer **15** in order to study the handedness of the helicates. Strong signals emerged at 485 nm and 438 nm in the CD spectra of **18**. It was thus proposed that the two ends of the molecule approach each other while forming the helicate. The handedness of the helicates deduced from the CD spectra was further substantiated by molecular modeling (Fig. 10).

Oligo(*m*-ethylenepyridine)s **19** and **20** were reported to self-assemble into triple-strand helicates in the presence of Cu(I) ion [93,94]. When ring-closing metathesis (RCM) was carried out under conditions that favored the triple helicate formation, random couplings took place among the six dangling terminal alkene groups. After dissociation with the copper ion, four different products (i.e., monomeric, dimeric, and trimeric cyclic as well as trimeric acyclic oligomers of **19**) were detected. This result validated the formation of triplexes (Fig. 11).

Another example of AEFS that binds to cations was poly(*m*-pyridinyleneethynylene-*alt*-*m*-phenyleneethynylene) **21**. This oligomer was also demonstrated to fold into helical conformation in polar solvent, and the induced helix could be further stabilized by protons or sliver ions, which were postulated to bind with the pyridine units [95] (Fig. 12).

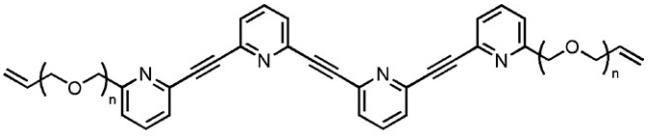

Fig. 11. Oligo(*m*-ethynylenepyridine)s **19** and **20** [93].

2.1.4. Anion-binding induced folding of oligoindoles

Investigations at oligoindoles linked by ethynylene units were reported by Jeong et al. [37,96]. According to molecular modeling, hexamer, and octamer of oligoethynylene indoles could assume a helically folded conformation with an inner cavity, the size of which was estimated to match well with that of a chloride anion. When solutions of oligoindoles **22**–**24** in CD_3CN were added with tetrabutylammonium chloride, downfield shifts of the N*H* signals in the ^1H NMR spectra evidenced hydrogen bond formation. This was accompanied with sharpening of the resonance signals, indicating the oligomers adopted more ordered structures when binding to the chloride. Meanwhile, aromatic CH resonances exhibited upfield shifting, which is in agreement of the occurrence of π–π stacking.

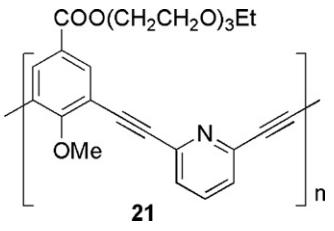

Fig. 12. Poly(*m*-pyridinyleneethynylene-*alt*-*m*-phenyleneethynylene) **21** [95].

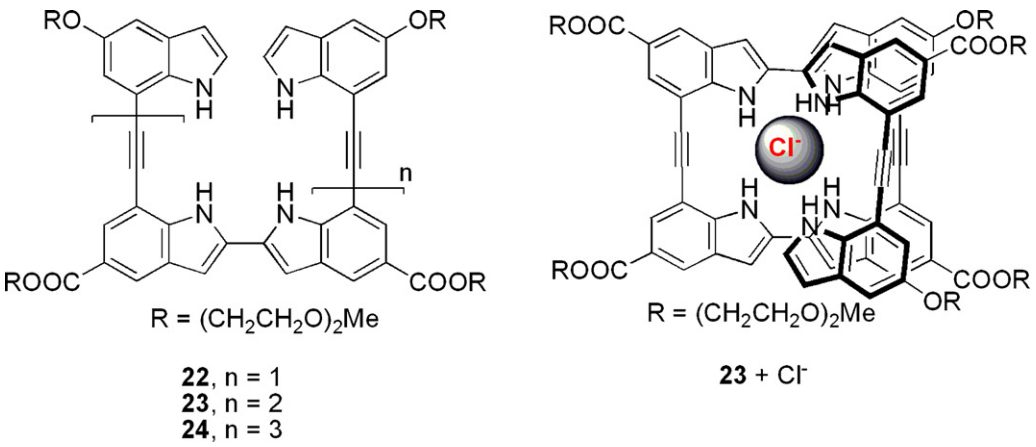

Fig. 13. Structures of ethynylene-linked indole tetramer **22**, hexamer **23**, and octamer **24** (left); chloride ion induced folding of the hexamer (right) [37].

Furthermore, a 2D ROSEY spectrum of hexamer **23** in the presence of 1 equiv. of Cl^- showed NOE correlations between hydrogen atoms which are stacked in proximity in the folded conformation [37]. Nonlinear least-square fitting of the UV titration curves gave binding constants of $2.1 \times 10^2\ M^{-1}$ and $2.3 \times 10^4\ M^{-1}$ for hexamer **23** and octamer **24**, respectively, in 1/9 (v/v) H_2O–CH_3CN solutions at 22 °C. With the Job plots, a binding stoichiometry ratio of 1:1 was determined for the oligoindole–chloride complexes (Fig. 13).

Then chiral groups (*R*)- or (*S*)-1-phenylethylamine units were introduced to both ends of oligoindoles via an amide linkage to facilitate the characterization of the foldamers using CD spectroscopy [97]. Upon binding to a chloride ion, (*S*, *S*)-oligoindole **25** exhibited a strong positive CD signal at 395 nm, while (*R*, *R*)-oligoindole **26** gave a mirror-image spectrum. Induced CD signals implied a preferential formation of a helical oligoindole with one handedness over the other in the folded conformation. On the basis of the theoretical calculations, one may conclude that the optimized structure of the (*P*)-helix of the (*S*, *S*)-oligoindole was less sterically crowded compared to the (*M*)-helix (Fig. 14).

Oligoindoles **27**–**30** with polar side chains were capable of binding anions in a mixed solvent of MeOH/DCM [98]. In addition to upfield shifting of the aromatic CH signals in the ^1H NMR spectra, bathochromic shift of the emission band accompanied with intensity quenching was observed in the fluorescence spectra, both of which supported the binding-induced folded conformation (Fig. 15). Association constants of oligomers **29** and **30** binding various anions were calculated on the basis of titration experiments monitored by fluorescence spectroscopy (Table 1).

Fusing the biindole unit into a rigid indolocarbazole structure forced the two NH groups to be oriented in the same direction. Such a structural modification was designed to enhance the anion-binding ability of oligomers **31**–**36** [99,100]. Solubility of indolocarbazole-based foldamers **34**–**36** in water was imparted by the carboxylate side groups. In D_2O, indolocarbazole trimer **36** adopts a non-aggregated but folded conformation, indicated by its concentration-independent ^1H NMR spectra and by comparison with the spectrum of monomer **34**. The existence of multiple hydrogen bonds between trimer **36** and various anions (F^-, Cl^-, and Br^-) in water was evidenced by changes in the chemical shifts of relevant protons in the ^1H NMR spectra. Association constants of trimer **36** with various anions in polar solvent D_2O, acquired from ^1H NMR titration experiments, decreased in the order of Cl^- ($65 \pm 2\ M^{-1}$) > F^- ($46 \pm 2\ M^{-1}$) > Br^- ($19 \pm 2\ M^{-1}$) at 24 °C. This order was different from that obtained from 4:1 (v/v) DMSO/MeOH solutions, which was $F^- > Cl^- > Br^-$. The disparity in the binding trend was attributed to the different competing energies of solvation in different media. Furthermore, binding affinity of the trimer for Cl^- was independent of the counterion (Li^+, Na^+, or K^+) (Fig. 16).

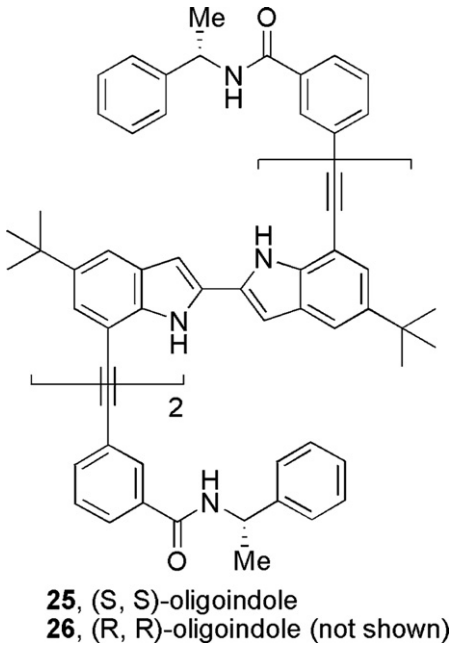

Fig. 14. Chiral oligoindoles **25** and **26** [97].

2.2. Foldamers as reactive sieves – toward synthetic enzyme

The cavitand foldamers are envisioned promising synthetic scaffolds for achieving the function of catalysis [13]. Guest binding

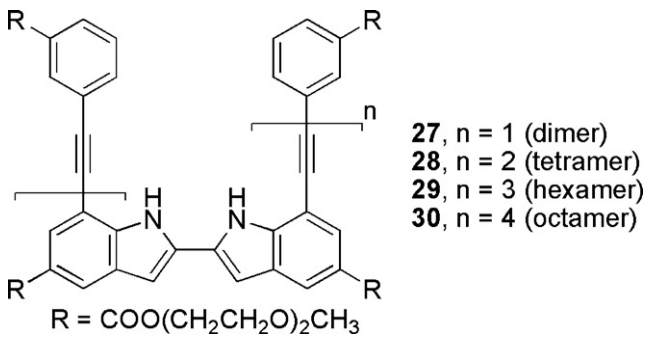

Fig. 15. Structures of oligoindoles **27**–**30** [98].

Table 1
Summary on association constants of foldamer-guest complexes.

Host	Guest	K_{ass} (M^{-1})	Solvent/T (K)	Characterization method	Reference
1b	(−)-α-Pinene	$3.1 \pm 0.18 \times 10^4$ $5.9 \pm 0.35 \times 10^4$ $1.0 \pm 0.06 \times 10^6$ $1.4 \pm 0.09 \times 10^6$ $1.2 \pm 0.01 \times 10^5$	H_2O/CH_3CN[a,b] (6:4) (7:3) (8:2) (9:1) (10:0)	CD	[81]
2	**5**	1.0×10^3	CH_3CN/r.t.	CD	[82]
7	**8**	$1.2 \pm 0.4 \times 10^3$	DCM/298	CD	[36]
9	**8**	$1.7 \pm 0.3 \times 10^2$ [c]$1.8 \pm 0.1 \times 10^3$	DCM/299 (0.0 equiv. H^+) (0.5 equiv. H^+)	CD	[83]
9	*o*-Octyl-β-D-Fru	$1.0 \pm 0.1 \times 10^2$ [c]$2.0 \pm 0.5 \times 10^4$	DCM/299 (0.0 equiv. H^+) (0.5 equiv. H^+)	CD	[83]
9	*o*-Octyl-β-D-Man	$3.3 \pm 0.5 \times 10^3$ [c]$7.2 \pm 1.3 \times 10^3$	DCM/299 (0.0 equiv. H^+) (0.5 equiv. H^+)	CD	[83]
9	*o*-Octyl-β-D-Gal	Too small [c]$2.2 \pm 0.4 \times 10^3$	DCM/299 (0.0 equiv. H^+) (0.5 equiv. H^+)	CD	[83]
11	Native hexoses	14 (D-mannose) 5.5 (D-fructose) 4.4 (D-allose)	H_2O/MeOH (10:1)/298 (10:1)/298 (10:1)/298	CD	[84]
13	**8**	$1.0 \pm 0.3 \times 10^2$ [d]$8.0 \pm 0.7 \times 10^2$ [e]$1.5 \pm 0.3 \times 10^3$	DCM/298 (TETA) (TETA-TFA)	CD	[89]
22	Cl^-	$1.3 \pm 0.1 \times 10^5$	CH_3CN/295	UV–vis	[37]
23	Cl^-	$1.2 \pm 0.1 \times 10^6$ $2.1 \pm 0.1 \times 10^2$	H_2O/CH_3CN (0:10)/295 (1:9)/295	UV–vis	[37]
24	Cl^-	$>10^7$ $2.3 \pm 0.2 \times 10^4$	H_2O/CH_3CN (0:10)/295 (1:9)/295	UV–vis	[37]
25	X^-	2.9×10^5 (Cl^-) 6.2×10^4 (Br^-) 2.6×10^2 (I^-) 4.4×10^4 (NO_3^-) 8.5×10^5 (N_3^-)	DCM/MeOH (99:1)/294	UV–vis	[97]
29	X^-	5.1×10^5 (F^-) 1.1×10^5 (Cl^-) 1.6×10^4 (Br^-) 4.0×10^3 (I^-) 8.5×10^4 (CN^-) 6.0×10^4 (N_3^-) 4.8×10^3 (NO_3^-) 2.9×10^4 (AcO^-)	DCM/MeOH (4:1)/297	Fluorescence	[98]
30	X^-	1.2×10^6 (F^-) 2.9×10^5 (Cl^-) 5.0×10^4 (Br^-) 2.1×10^4 (I^-) 1.1×10^5 (CN^-) 1.2×10^5 (N_3^-) 8.0×10^4 (NO_3^-) 9.4×10^4 (AcO^-)	DCM/MeOH (4:1)/297	Fluorescence	[98]
31	Cl^-	11	DMSO/MeOH (4:1)/297	^1H NMR	[99]
32	Cl^-	5.6×10^2	DMSO/MeOH (4:1)/297	^1H NMR	[99]
33	X^-	1.8×10^5 (F^-) 3.7×10^4 (Cl^-) 1.4×10^3 (Br^-) 86 (I^-)	DMSO/MeOH (4:1)/297	Fluorescence	[99]

Table 1 (*Continued*)

Host	Guest	K_{ass} (M^{-1})	Solvent/T (K)	Characterization method	Reference
36	X^-	46 ± 2 (F^-) 65 ± 2 (Cl^-) 19 ± 2 (Br^-) <1 (I^-)	D_2O/297	^1H NMR	[99]

[a] The respective solvent composition is noted in the parentheses.
[b] Experiment temperature was not reported; presumably measured at room temperature.
[c] Polymer **4** with 0.5 equiv. TFA (relative to repeating units).
[d] Formal binding constant in the presence of TETA.
[e] Formal binding constant in the presence of TETA and TFA.

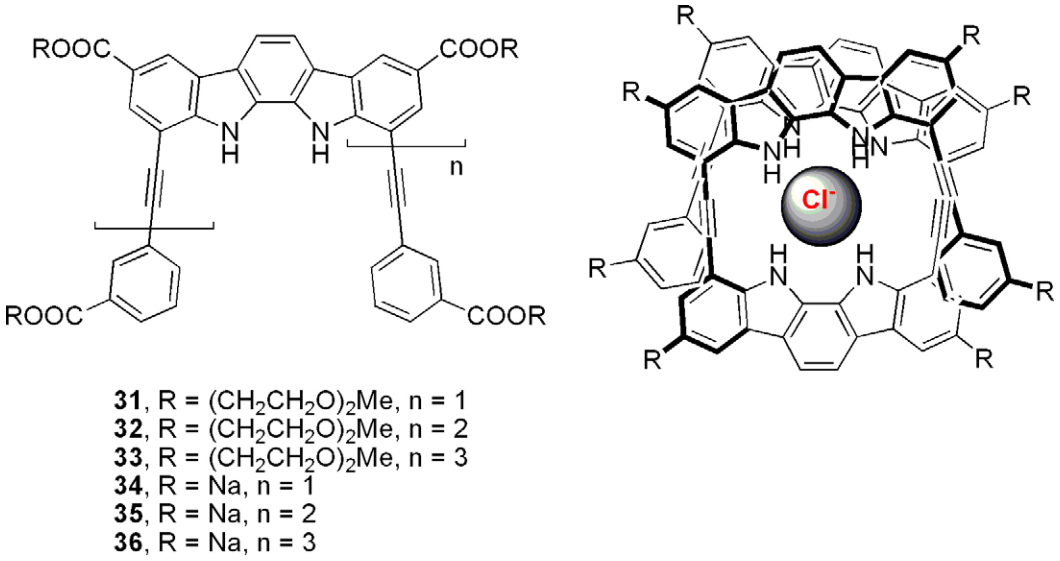

31, R = $(CH_2CH_2O)_2Me$, n = 1
32, R = $(CH_2CH_2O)_2Me$, n = 2
33, R = $(CH_2CH_2O)_2Me$, n = 3
34, R = Na, n = 1
35, R = Na, n = 2
36, R = Na, n = 3

Fig. 16. Structures of ethynylene-linked indolocarbazole oligomers **31**–**36** (left) and a trimer binding a chloride ion (right) [99].

is among the first series of processes to be realized in developing artificial enzymes that perform chemical transformations. The *m*PE foldamer is capable of molecular recognition with the cavity inside its helically folded architecture (vide ante). In addition to the capability of binding a guest (or substrate), to accomplish the transformation function, the cavity evidently needs to serve as an "active site" of "turn-over" capacity. The *m*PE oligomers are advantageous for this task by virtue of their modularly constructed chain structures. Namely, they can be chemically modified conveniently and functionalized without significantly disrupting the folded conformation. Moore and coworkers have ventured down the path and made seminal progress.

The phenylene ethylene backbone was decorated with functional groups in order to modify the internal surface of the cavity and accomplish designed chemical transformation in the folded conformation. A pyridine unit was incorporated into the middle of a phenylene ethylene chain and proven not to significantly destabilize the helical conformation in acetonitrile [27]. It was not surprising to find that the basicity of the pyridine unit could be easily modulated by changing the substituents on the pyridine ring in oligomers **37**–**41** [101]. In the folded conformation, the basicity was also slightly influenced by the interaction between pyridine and phenyl rings, as a result of more compact stacking thereof than in the unfolded state (Fig. 17).

Under the folded conformation, the lone-pair electrons of the pyridine unit should be directed to the interior of the cavity and thus capable of nucleophilic attack on the guest molecule bound inside the cavity. Pyridine–containing phenylene ethylene oligomers **42**–**49** of different chain lengths were used to probe this property. It was discovered that under the folded conformation the methylation (by methyl iodide) rate of the pyridine unit in oligomers that contained more than eight repeat units was much faster compared to that in oligomers of a shorter chain length [102,103]. In contrast, a control experiment showed that under otherwise the same methylation conditions the reaction rate in $CHCl_3$ was nearly independent of the chain length. This result unambiguously indicated that folding, which only happened with longer oligomers in polar solvent, drastically accelerated the methylation reaction (Fig. 18).

In a subsequent study, a competitive binding/inhibition experiment excluded the possibility that a foldamer was binding with more than one guest molecule prior to the methylation. It was thus proposed that constraining the methylation reagent in close proximity of the reactive moiety was the primary cause for the observed rate enhancement of the methylation [104].

Apparently, the molecular recognition ability of the foldamers would be influenced by both the size and shape of the guest molecule as well as the cavity interior surface features, and the binding strength would in turn affect the outcome of the guest-involved chemical transformation. Hence, different guest

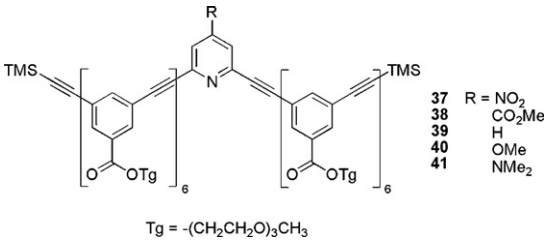

Fig. 17. Chemical structures of compounds **37**–**41** [101].

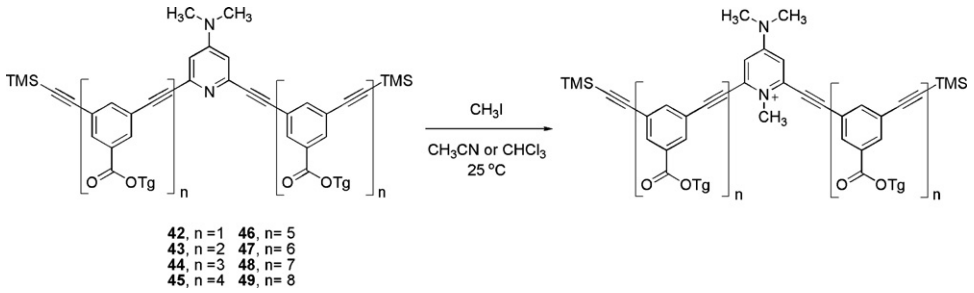

Fig. 18. Methylation of pyridine-containing *m*PE oligomers **42**–**49** of different lengths [102,103].

molecules and oligomers offering varied–sized cavities were systematically investigated in terms of their reactive sieving properties [105,106]. Again, methylation of the pyridine-containing *m*PE oligomers was employed as a probing reaction platform. The cavity of the foldamers was modulated by chemical modification of the oligomer structure (**50**–**53**). A series of methyl sulfonates, bearing linear or branched alkyl chains, were synthesized to be the methylation reagents (Fig. 19).

A few important conclusions were drawn from this study. First, with a certain methyl sulfonate, the methylation rate typically increased with the increasing length of the oligomers. This was possibly a result of the more stable helical conformation of the longer oligomers. Secondly, the flexible nature of the folded structure of oligo(*m*PE) allowed it to accommodate different guest molecules. Nonetheless, the reaction rate was sensitive to the size and shape of the guest molecule. For sulfonates of linear alkyl chains, the methylation reaction proceeded faster with the reagents of longer tails. This was probably due to the more significant solvophobic effect of the longer alkyl tails. The situation was more sophisticated for the branched sulfonates, and sieve-like behaviors were observed more pronouncedly with this series. Both size and shape of the sulfonates played a role, although it appeared that the reactivity is governed more by the shape than by the size. The orientation of the reactive groups inside the cavity was particularly relevant. Also, the variation trend of the reaction rate did not perfectly match the "55% rule" conferred from alternative supramolecular systems [107]. End-functionalized oligomers **54** showed no reactive sieving ability when it was subjected to different methyl alkylsulfonates [106]. This could be explained by the molecular dynamics simulation studies, which indicated that more significant conformational fluctuations occur with the end of the chain [108] (Fig. 20).

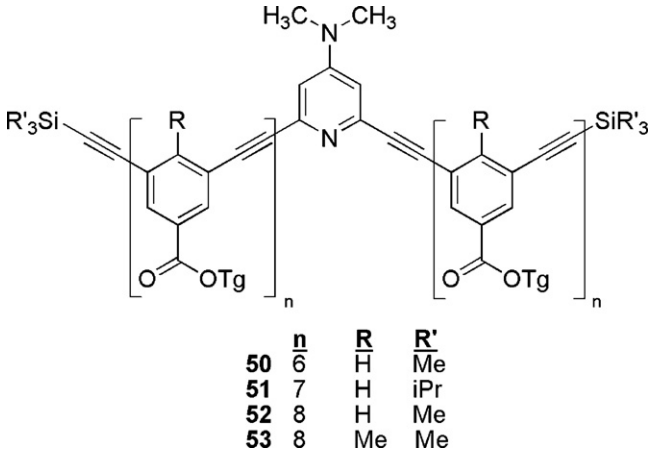

Fig. 19. Chemical structures of oligomers **50**–**53** [105,106].

2.3. Photo-responsive AEFS

While solvent properties have been widely manipulated to enable the folding transition of foldamers, incorporation of a photoisomerizable unit into the backbone elegantly establishes an effective, reversible control over the helix–coil transition of a foldamer. Hecht et al. reported the photoswitchable foldamers **55**–**57** by harnessing the photoisomerizable azobenzene unit [109,110].

An azobenzene unit was incorporated into the center of the oligo(*m*PE) backbone via a varied connectivity (Fig. 21). The length of the two oligo(*m*PE) arms appended to the azobenzene unit was specifically chosen so that they were not long enough to adopt a helical conformation independently, but when the central photoisomerizable unit adopted a proper configuration, the overall molecular chain could fold into a helical conformation. Specifically, in the case of 'turn-on' helix, oligomers **55** and **56** were able to fold into a stable helical conformation when the azobenzene was in the *cis* state, while the *trans*-azobenzene disrupts the helix. In contrast, the 'turn-off' helix **57** could fold with azobenzene in the *trans*-conformation and unfold with the azobenzene in the *cis*-conformation. For oligomer **57** with chiral side chains, using UV–vis and CD spectroscopies, a reversible helix–coil transition was observed to take place and governed by the *cis–trans* transformation of the azobenzene unit, the latter of which was controlled by irradiation of light with proper wavelength or suitable thermal conditions [111].

2.4. Incorporating metal ions into the mPE backbone

In regard to the goal of enzyme mimicry, incorporating metal ions into foldamer systems is of particular interest in recent years, since metal ions serve as active centers in biological systems such as hemoglobin [112], carbon monoxide dehydrogenase [113], etc.

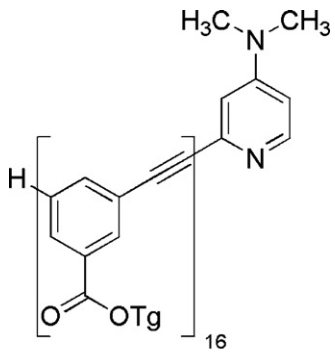

Fig. 20. Chemical structures of compound **54** [106].

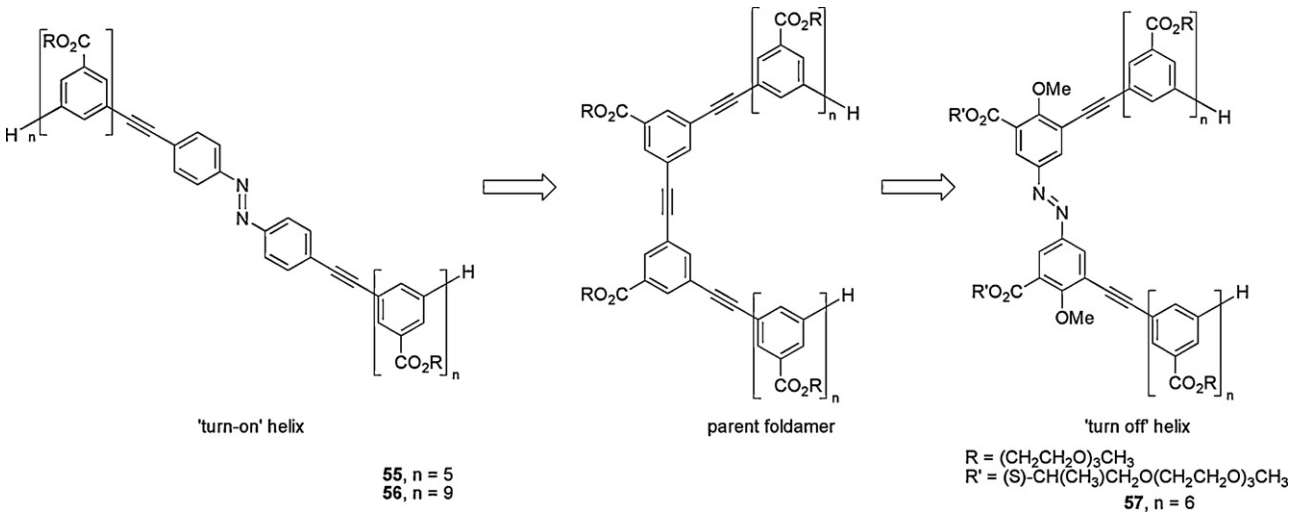

Fig. 21. Chemical structures of compounds **55**–**57** [109,110].

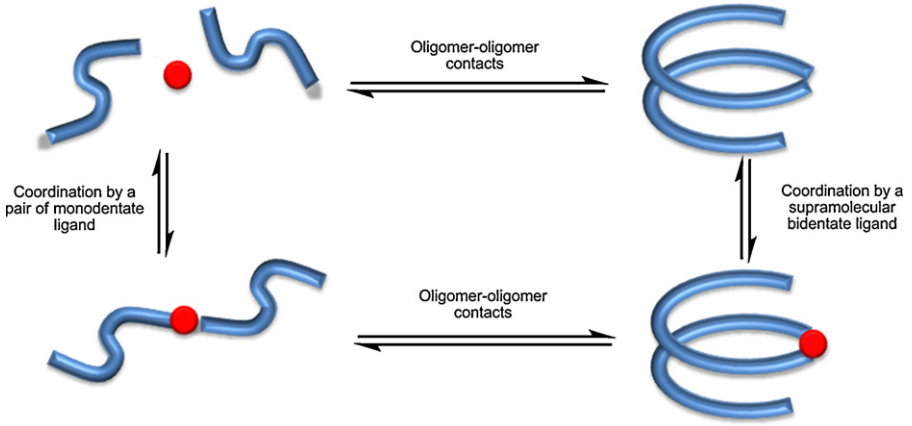

Fig. 22. Coordination-enabled folding of *m*-phenylene ethylene foldamers [114]. (Reproduced with permission from Ref. [114].)

By introducing metal ions into foldamer scaffolds, potential applications such as supramolecular catalysts, enzyme mimics, and so on, might be achieved. Relevant investigations were carried out by a number of research groups.

Based on calculations, the distance between two nitrogen atoms of a *trans* pyridine–Pd(II) complex is very close to the average distance between two ipso carbons of diphenylethylene structures, making the *trans* pyridine–Pd complex unit a suitable segment to be inserted into the *m*PE foldamer backbone without significant disturbing the helical conformation [114]. Based on UV–vis absorption studies, pentamer **60** was unable to fold. Yet, upon coordination to a Pd ion the oligomer complex exhibited a stable, folded structure. Such coordination-enabled folding was reasonably explained by the additional intramolecular aromatic stacking interactions resulting from the elongated oligomer chain length upon complexation (Fig. 22).

Additionally, on the basis of ^{1}H NMR spectra the folded conformation of complex **60**–Pd–**60** was suggested to be more stable than that of complex **58**–Pd–**58**. Thermodynamic parameters obtained by isothermal calorimetry titrations between oligomers **58**–**62** and *trans*-$PdCl_2(CH_3CN)_2$ further supported the postulation that coordination was strengthened by the additional free energy gained from folding of the elongated oligomer chains. Furthermore, bis-functionalized oligomers **63**–**65** were synthesized. For sequences **63** and **65** a coordination-entailed polymerization reaction occurred upon addition of *trans*-$PdCl_2(CH_3CN)_2$ into the system [115]. The polymerization was proven to proceed with a nucleation–elongation mechanism [116–119]. Specifically, once the critical chain length that enables folding was reached by the growing species in the system, subsequent chain extension became thermodynamically more favored due to the additional free energy gained by the folding and stacking (Figs. 23 and 24).

In an independent study, Lee et al. reported coordination polymers based on bispyridine terminated *m*PE ligands **66**–**69** coordinating to silver ions [120]. The chain conformations of the coordination polymers were pronouncedly affected by the counterions (Fig. 25).

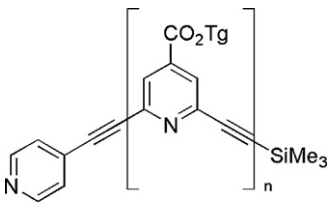

Fig. 23. Chemical structures of compounds **58**–**62** [114].

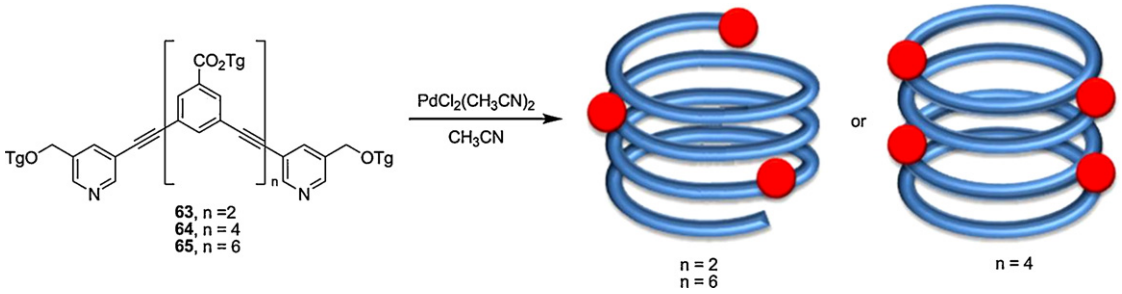

Fig. 24. Coordination induced folding of compounds **63**–**65** [115]. (Reproduced with permission from Ref. [115].)

Specifically, coordination polymers **66** and **67** formed pentagonal helices, with the interior cavity occupied by counterion NO_3^- and BF_4^- in the solid state, respectively. Interestingly, when the counterion became $CF_3SO_3^-$, two bent-shaped bipyridine ligands coordinated with two sliver ions and formed a macrocycle, instead. These macrocycles then self-assembled into a columnar phase. As the size of the counteranion further increased to $C_3F_7SO_3^-$, coordination polymer **69** adopted an extended zig-zag chain conformation in the solid state. This observation was attributed to the particularly large size of $C_3F_7SO_3^-$ anion, which was presumably too big to fit in the cavity formed by the folded chains. The polymer chains could also be tuned to transform from the extended zig-zag conformation to folded double helices simply by replacing the metal ion bridge from *trans* palladium dichloride to *trans* copper dichloride (i.e., changing from polymer **70** to polymer **71**). This duplex formation was attributed to the copper-chloride dimeric interactions present between the two composing polymer chains along the axle of the formed double helix [121] (Fig. 26).

Phenanthrylene ethynylene ligand **72** bearing two terminal pyridine units also formed a folded helical polymer by coordinating to silver trifluoromethanesulfonate. More interestingly, such a coordination polymer could undergo a reversible extension–contraction motion [122]. This motion of the polymer was governed by the LCST (lower critical solution temperature) of the oligo(ethylene oxide) chain. Below the LCST, the dendritic ethylene oxide side chains were well hydrated and existed in relatively extended, random coil conformations, which entails less steric repulsion among side chains. As the temperature was raised to above the LCST, the dendritic ethylene oxide chains became poorly hydrated and collapsed into globules. The increased bulkiness and repulsions between adjacent globular side chains therefore

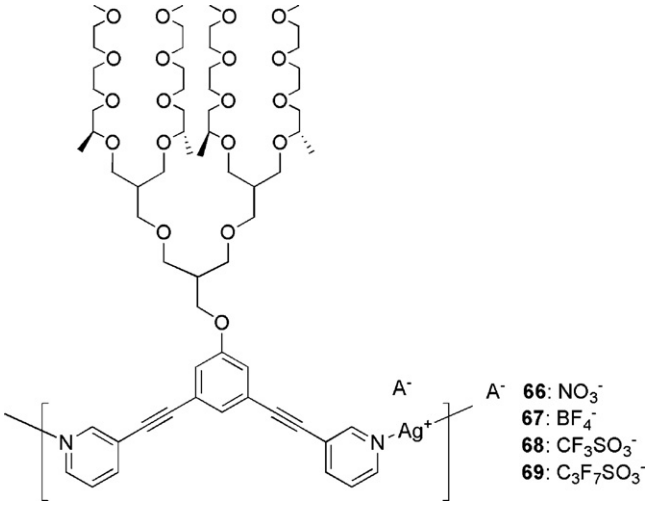

Fig. 25. Chemical structures of compounds **66**–**69** [120].

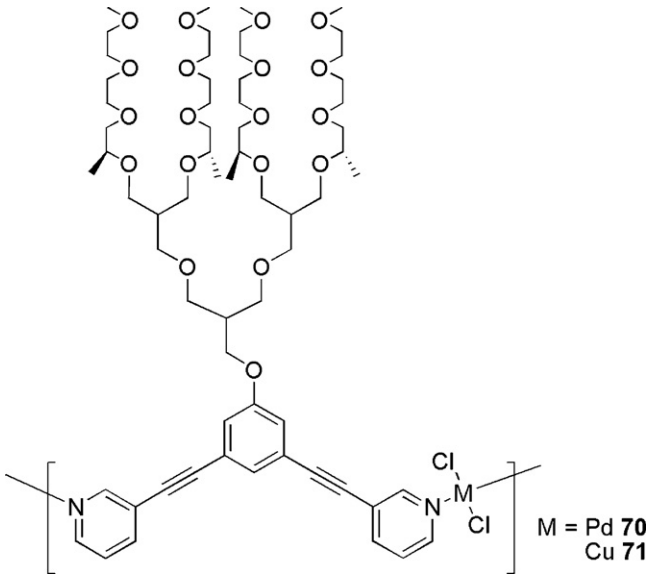

Fig. 26. Chemical structures of compounds **70** and **71** [121].

stretched the helical pinch. The occurrence of such a process was confirmed by fluorescence resonance energy transfer (FRET) and 2D NMR experiments (Fig. 27).

2.5. Ortho-phenylene ethynylene foldamers

It can be imagined that, similar to the oligo(*m*-phenylene ethynylene) systems, given suitable conditions oligo(*o*-phenylene ethynylene)s should also be able to adopt helical conformation, with three phenylene ethynylene repeat units per turn. Computational studies predicted that, like *m*PE oligomers, under solvophobic conditions folding of oligo(*o*-phenylene ethynylene) (*o*PE) should be enthalpy-favored [123], accompanied by an

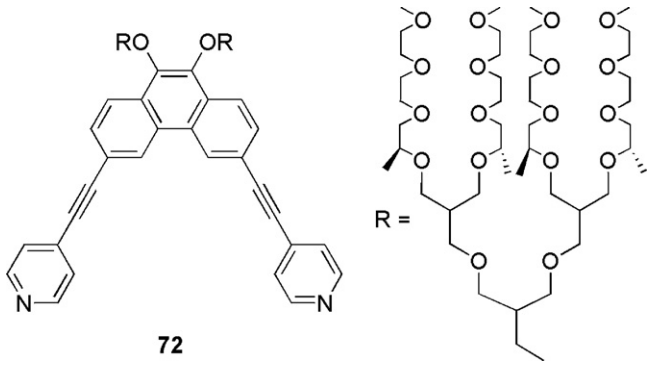

Fig. 27. Chemical structure of compound **72** [122].

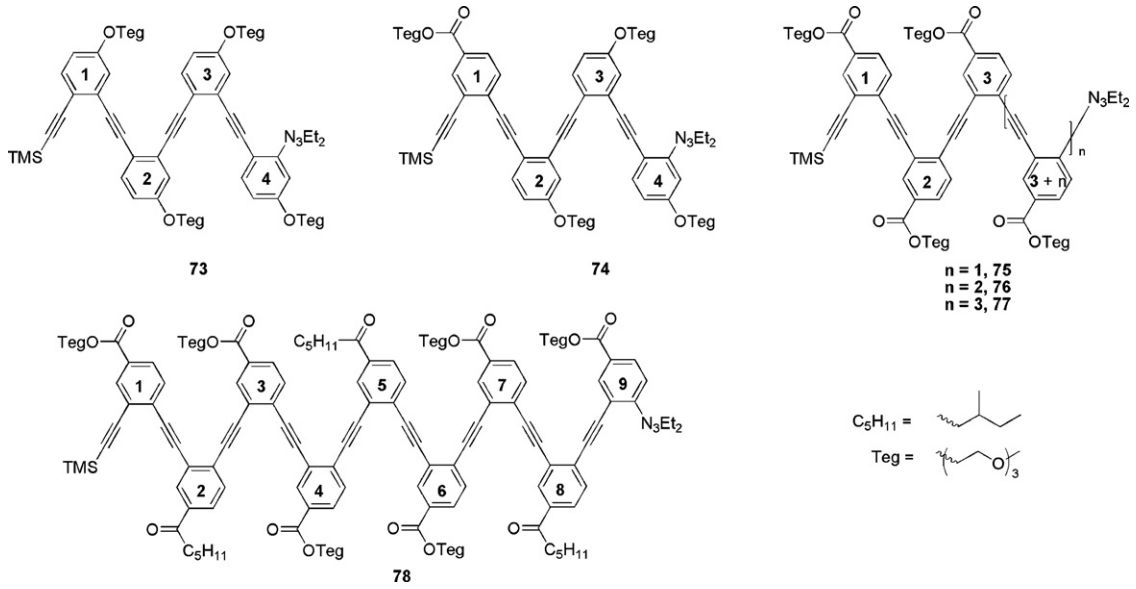

Fig. 28. Chemical structures of compounds **73**–**78** [38,127–129].

entropy loss. Nonetheless, while the folding properties of *m*PE systems have been thoroughly investigated, only a few *o*PE oligomers were synthesized and reported in earlier studies [124–126].

With 1D and 2D NMR spectroscopies, Tew and coworkers confirmed that in polar solvents *o*PE oligomers **73**–**75** could fold into compact helical conformations with three phenylene units a turn [38]. 1D ^{1}H NMR showed that for these molecules the resonances of hydrogen atoms on phenyl rings 1 and 4 shifted upfield when the polarity of the solvent increased, while the chemical shifts of hydrogen atoms on rings 2 and 3 remained constant (Fig. 28). These results were consistent with a folded conformation, in which the chemical environment of protons on rings 1 and 4 changed evidently upon folding, as a result of face-to-face π–π stacking of these two rings. Strong NOE between the TMS protons and protons on ring 3 of oligomer **74** was observed in acetonitrile, indicating that ring 1 was stacking with ring 4 with the TMS group lying in proximity with ring 3. Similarly, oligomer **75** in acetonitrile exhibited strong NOE between TMS protons and methyl protons of triazene group. NOESY spectra of oligomer **74** and ROESY spectra of oligomer **75** indicated that rings 1 and 4 stacked in a face-to-face fashion, which further confirmed the proposed helical conformation of *o*PE foldamers in polar solvents.

Due to the distinct structural geometry, the minimum chain length for *o*PEs to fold was 4 repeat units, which is a much shorter critical length than that of *m*PE foldamers. When the length of *o*PE foldamer increases, such as for oligomers **76** and **77**, the possible conformations of the folded state become more complex. By making assignment of the spin system for the homo-*o*PE foldamers [127], Tew et al. clarified the folded conformation of hexamer **77** [128]. Chemical shifts of protons on the central ring of pentamer **76** remained constant; other protons on rings 1, 2, 4, and 5 shifted upfield with increased solvent polarity; whereas protons of all 6 phenyl rings in the hexamer shifted upfield when solvent polarity increased. Such changes in the chemical shifts of phenylene protons underlined that the oligomers folded into a helical conformation in the polar solvents with 3 PE units per turn. The conclusion was further supported by the ROSEY spectra. *o*PE oligomers up to nonamer **78** were synthesized and proven to be capable of switching between folded and unfolded states in different solvents [129]. A polymer of *o*PE reported by Khan and Hecht also exhibited evidence for chain folding into a helical conformation [130].

2.6. *oPE-alt-pPE folding system*

Oligo(*o*-phenyleneethynylene-*alt*-*p*-phenyleneethynylene) **79** (Fig. 29) with alkyl side chains was synthesized by Zhao and coworkers and also assumes a folded conformation in apolar solvent cyclohexane by UV–vis and fluorescence emission characterizations [39]. The purpose of the design was to achieve a foldable, conjugated chain molecule, and thereby to explore a novel organic semiconducting material with unique charge/energy transporting properties. It can be imagined that in a helically folded conjugated molecule (e.g., oligomer **79**) the effective direction of charge/energy transport via π-conjugation along the aromatic backbone and that via π–π stacking can be unified to be along the helix main axis. This is in great contrast with the situation with conventional linear, conjugative chain structures, in which the directions of charge/energy transport affected by these two types of interactions are orthogonal with each other.

A seemingly simple modification of inserting a *p*PE units between every *o*PE segment was a critical design factor to ensure the conjugative property of the oligomer, which is indispensable for semiconductive systems. By extending the distance between the *o*PE units, torsional strain in the folded oligo(*o*PE)s can be significantly released and the coplanarity of adjacent aromatic

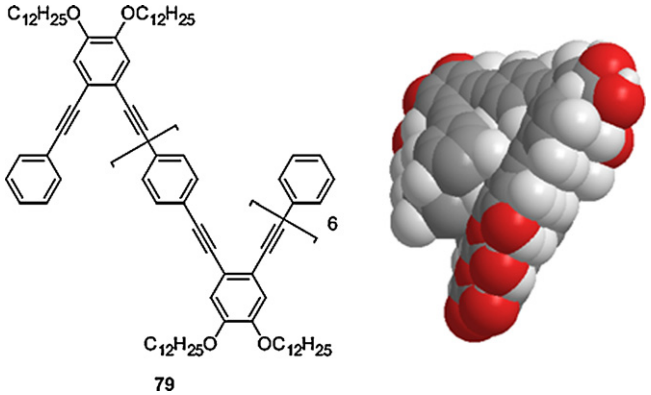

Fig. 29. Chemical structure of an oligo(*o*-phenyleneethynylene-*alt*-*p*-phenyleneethynylene) and a model of it in the folded conformation (alkyl side chains replaced with hydrogen for clarity) [39].

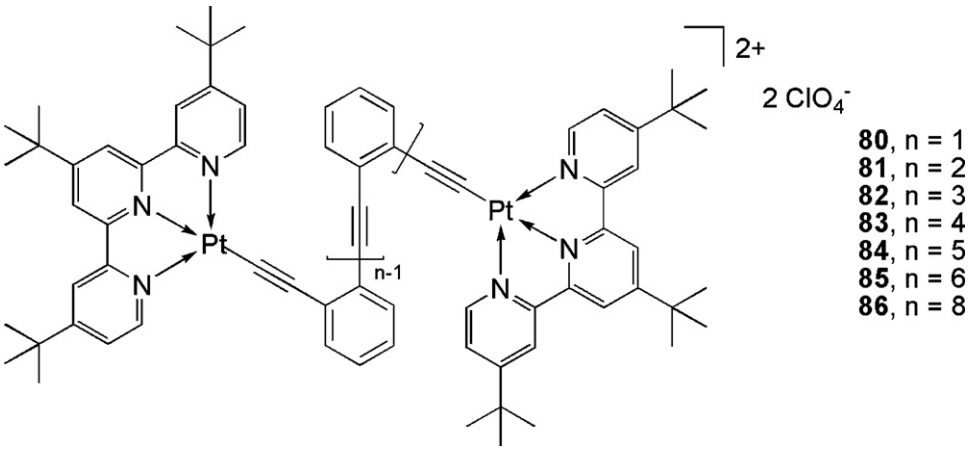

Fig. 30. Chemical structures of compounds **80**–**86** [131].

units can be greatly improved. Thereby, electronic coupling and π-conjugation along the backbone can be more effective relative to oligomers comprising sheerly *o*PE units. The reported oligo(*o*PE-*alt*-*p*PE) was designed as a primitive model of a foldable conjugated chain molecule, for the purpose of interrogating the folding capability. Replacing the *p*-phenyl units with alternative aromatic units with better semiconductive properties will furnish systems with superior performance.

2.7. *oPE oligomers end-capped with Pt complexes*

Che et al. reported a series of *ortho*-phenylene ethylene foldamers end-capped with terpyridyl-platinum(II) complex units **80**–**86**. The binuclear terpyridyl-platinum(II) complexes **82**, **84** and **85** were confirmed to adopt partial-helical conformations in the solid state by single crystal X-ray crystallography [131], although single crystals of **83** and **86** suitable for X-ray diffraction analysis were not obtainable. The phosphorescence of these terpyridyl-platinum(II) complex end-capped foldamers showed an interesting solvatochromic property. Specifically, the emissions of complexes **82**–**86** were red-shifted and the intensity was amplified with an increasing water percentage in the aerated water–acetonitrile binary solvent. This observation was postulated to be a result of enhanced intermolecular aggregation and/or intramolecular folding of the oligomers through π–π interactions and/or Pt–Pt interactions. Additionally, dynamic light scattering and transmission electron microscopy studies revealed that these oligomeric binuclear platinum(II) complexes aggregated into nanosized particles in acetonitrile/water mixed solvents (Fig. 30).

2.8. *1,8-Anthrylene ethynylene foldamers*

1,8-Anthrylene with a turning angel of 180° was recently introduced by Toyota et al. [132] as a building block into an arylene ethynylene foldamer. Compared with other aromatic units employed to construct foldamers, 1,8-anthrylene possesses unique geometric and electronic properties.

Based on the results from studies on 1,8-anthrylene ethynylene macrocycles **87** and **88** [132–134], interactions between stacked anthracene units were not strong enough to stabilize the conformer of D_2 symmetry; instead, a square prism was observed. The energy barrier between two chiral diamond prisms through skeletal "swing" was estimated to be 38 kJ mol^{-1} by varied-temperature ^{1}H NMR (Fig. 31).

Analogously, as lacking specific secondary interactions such as the solvophobic effect to stabilize the folded conformation, oligomeric 1,8-anthrylene ethynylenes did not exhibit a stable folded conformation in solution [1,70–80]. However, anthracene is known to be able to dimerize via a [4+4] cycloaddition, and the reaction can be reversed under suitable thermal conditions. This feature thus was exploited as a unique driving force to achieve folding, i.e., a reversible chemical reaction was harnessed to enable folding. Specifically, acyclic 1,8-anthrylene ethynylene trimer **89** dissolved in degassed benzene was irradiated with a high pressure Hg lamp. An intramolecular cycloaddition reaction was initiated and the oligomer was thus locked in a folded state through covalent bonding. Subsequently, by heating the solid-state sample of the photochemical adduct, a retro-cycloaddition took place. But the trimeric 1,8-anthrylene ethynylene was retained in the folded conformation in the solid state. Dissolving this sample in chloroform released the oligomer back to the unfolded state [135] (Fig. 32).

2.9. *Helical structures of mPE polymers in thin films*

Helical structures of *m*PE with a twist sense bias induced by chiral side chains were first reported in 1999 [136]. More recently, helices of one-handed twist sense were reported for *m*PE foldamer **90** [137]. In this case, chiral D-menthoxy substituents were appended to the phenylene units through an ester linkage and used to induce a preferred handedness of the helical structure. According to the CD spectra, the chirality of these one-handed helices was maintained in spin-coated films. Furthermore, *in situ* de-substitution of the chiral substituents in the film was accomplished by immersing the membrane into a KOH solution and then acidifying it with HCl. The completion of the reaction was confirmed by IR spectroscopy and gravimetry. CD spectrum recorded

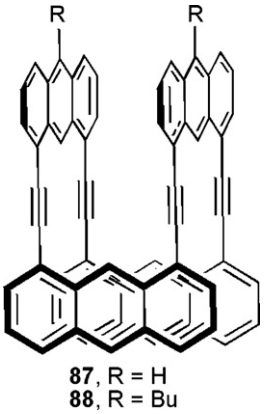

Fig. 31. 1,8-Anthrylene ethynylene macrocycles **87** and **88** [132–134].

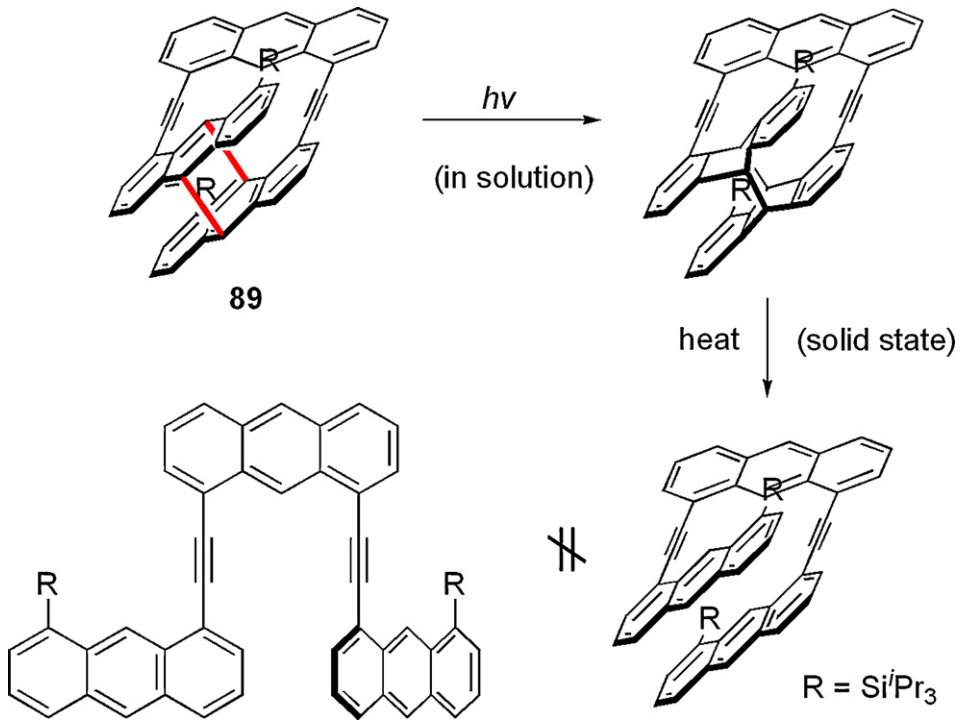

Fig. 32. Folding and unfolding of 1,8-anthrylene ethynylene oligomer **89** driven by photo-induced dimerization [135].

for the de-substituted polymer film was similar to that of the original spin-coated film, indicating helices with the same handedness were reserved after cleavage of the chiral side groups (Fig. 33).

Poly(*m*PE-*alt*-*p*PE) **91**–**93** bearing glycine derivative side chains were synthesized via Sonogashira coupling between *p*-diethynylbenzene and a diiodo substituted *m*-phenylene monomer [138]. Specific rotation, UV–vis and CD spectra confirmed that a helical conformation with predominantly one-handed twist sense was adopted by these polymers in nonpolar solvents and the condensed state. Intramolecular hydrogen bonds between amide groups were revealed by solution state IR spectra to be present between adjacent turns in the helices and believed to help stabilize the helix. The apparently slower H-D exchange rate of polymer **92** compared to that of its monomer further supported the existence of such hydrogen bonds between amide groups in the helical conformation (Fig. 34).

2.10. Foldable phenylene ethynylene polyelectrolytes

Poly(*m*PE-*alt*-*p*PE) electrolytes **94** and **95** were synthesized and studied by Schanze and coworkers [139,140]. Ionic functional groups were tethered to the polymer backbone by relatively short linkages, which made polymers **94** and **95** soluble in polar solvents. On the basis of the UV–vis absorption and fluorescence spectra of these polymers in a series of MeOH/H_2O mixed solvents with varied compositions, a coil (in MeOH) to helix (in H_2O) transition was suggested to occur with the polymer chain, similar to those observed with *m*PE oligomers of non-ionic side chains [4,9,10,26,64,136]. The helical conformation of polyelectrolyte **95** was further verified by CD spectrum. Remarkably, both polymers **94** and **95** were able to bind metallo-intercalator $Ru(bpy)_2(dppz)^{2+}$ in the folded helical conformation, which was considered analogous to $Ru(bpy)_2(dppz)^{2+}$ binding DNA via intercalation [141]. More significant fluorescence quenching was observed for polyelectrolyte **94** in the folded conformation than in the disordered conformation. This was explained due to greater exciton diffusion length or more efficient quencher–polymer interaction in the former state (Fig. 35).

Water-soluble fluorene-containing poly(arylene ethynylene) electrolytes **96**–**99** were also obtained via Sonogashira coupling reactions [142]. *Meta*-phenylene units were incorporated as nonlinear building blocks, while ammonium functionality made the polymers soluble in water. As the composition of the *meta*-phenylene unit increased from **96** to **98**, a gradual transition from random coil to helix was observed, shown by the UV–vis absorption spectra. However, likely due to the steric and electronic repulsion among the ammonium-functionalized side chains, tightly folded

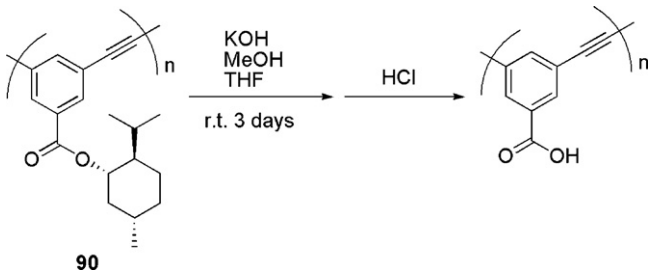

Fig. 33. Chirality of *m*PE polymer **90** immobilized in thin film [137].

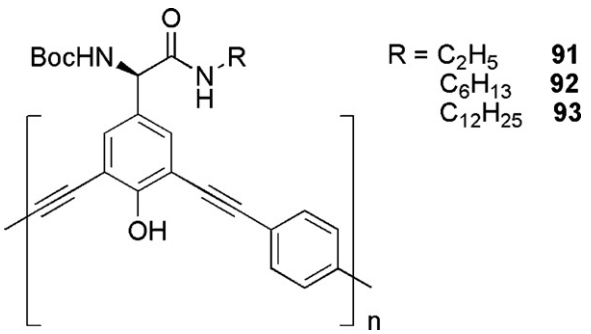

Fig. 34. Chirality immobilized in thin film of *m*PE polymers **91**–**93** [138].

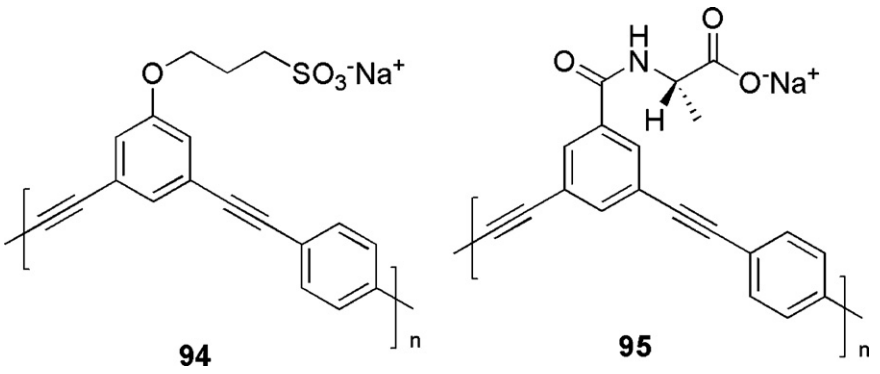

Fig. 35. Poly(*m*-phenylene ethynylene)s polyelectrolytes **94** and **95** [139,140].

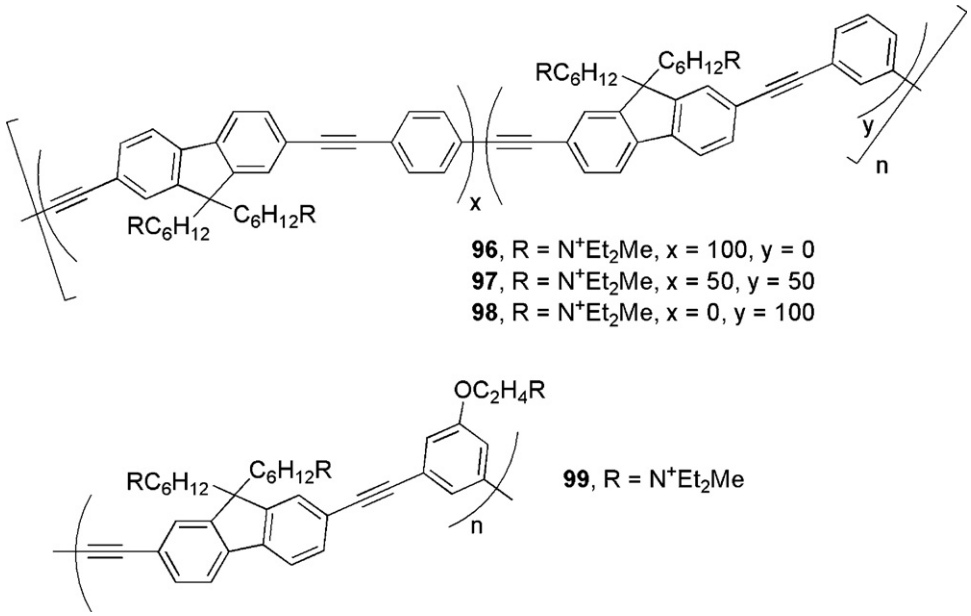

Fig. 36. Water-soluble fluorene-containing poly(arylene ethynylene)s **96**–**99** [142].

helical conformation was disfavored in these polymers. Nonetheless, iron–sulfur protein induced fluorescence quenching was more pronounced for the polymers with more features of helical conformation, which again resulted either from greater exciton diffusion length in the more compact helical conformation, or from better spatial interaction between the polymer and iron–sulfur protein secondary structure [142] (Fig. 36).

The above studies elucidated the potential advantages for relevant foldamers to be applied as fluorescence-based sensory materials.

2.11. Foldable copolymer

Stereo-regular poly(propylene oxide) (PPO) chains were introduced into poly(phenylene ethynylene) system to prepare novel chiral, amphiphilic block- and graft-copolymers **100** and **101** [143]. Despite the presence of the long, bulky PPO segments, UV–vis absorption and CD spectra indicated that both PE segments in the copolymers were capable of folding in polar solvents. This work presented a new approach to incorporating chiral elements into rod-coil block- and graft-copolymers (Fig. 37).

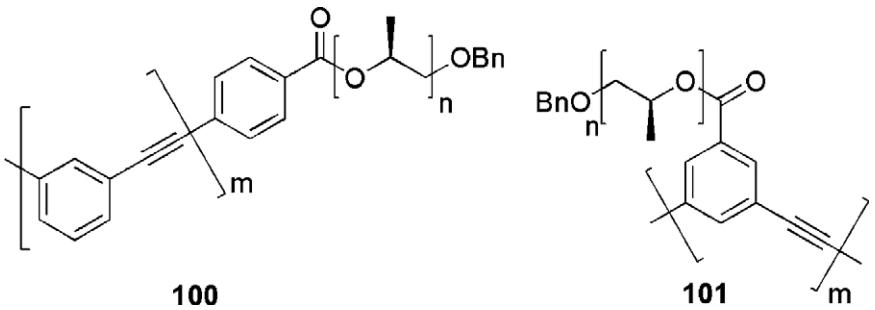

Fig. 37. Chiral block-copolymer **100** and graft-copolymer **101** containing poly(arylene ethynylene) segments [143].

3. Outlook

The above research unambiguously demonstrated that vast progress has been made at developing synthetic folding scaffolds using arylene ethynylene building blocks. Disregard the fact that these efforts were either devoted to modifying previously established foldable backbones into more complex systems, or they were made at constructing foldable architectures using newly designed and synthesized chemical building blocks, ultimately, bestowing functions to these AEFS has clearly become an essential focus. In addition to the achievement of relatively simple function of binding small molecules or ions, more sophisticated task of exploiting the binding cavity as a reactive site for chemical transformation has also been accomplished. Further upgrade of the reactive site into a catalytic center warrants the studies on how to realize, e.g., preferential binding of the substrate over product, as well as establishing the turn-over function. Besides the attractive goal of developing synthetic enzymes, alternative applications of functional AEFS as sensors or optoelectronic materials have also emerged. Evidently, vast opportunities exist for AEFS to serve as a unique, conveniently tailored, and versatile synthetic platform for studying and developing various functional systems.

Acknowledgements

Acknowledgement is made to the National Basic Research Program (2007CB808000) from the Ministry of Science and Technology and National Natural Science Foundation of China. We thank the students and colleagues for valuable discussion during the preparation of the manuscript.

References

[1] S. Hecht, I. Huc (Eds.), Foldamers: Structure, Properties and Applications, Wiley-VCH, Weinheim, 2007.
[2] S.H. Gellman, Acc. Chem. Res. 31 (1998) 173.
[3] K.D. Stigers, M.J. Soth, J.S. Nowick, Curr. Opin. Chem. Biol. 3 (1999) 714.
[4] D.J. Hill, M.J. Mio, R.B. Prince, T.S. Hughes, J.S. Moore, Chem. Rev. 101 (2001) 3893.
[5] R.P. Cheng, S.H. Gellman, W.F. DeGrado, Chem. Rev. 101 (2001) 3219.
[6] A.R. Sanford, B. Gong, Curr. Org. Chem. 7 (2003) 1649.
[7] R.P. Cheng, Curr. Opin. Struct. Biol. 14 (2004) 512.
[8] I. Huc, Eur. J. Org. Chem. 2004 (2004) 17.
[9] C.R. Ray, J.S. Moore, Adv. Polym. Sci. 177 (2005) 91.
[10] M.T. Stone, J.M. Heemstra, J.S. Moore, Acc. Chem. Res. 39 (2006) 11.
[11] A. Violette, S. Fournel, K. Lamour, O. Chaloin, B. Frisch, J.P. Briand, H. Monteil, G. Guichard, Chem. Biol. 13 (2006) 531.
[12] A.D. Bautista, C.J. Craig, E.A. Harker, A. Schepartz, Curr. Opin. Chem. Biol. 11 (2007) 685.
[13] R.A. Smaldone, J.S. Moore, Chem. Eur. J. 14 (2008) 2650.
[14] C.M. Goodman, S. Choi, S. Shandler, W.F. DeGrado, Nat. Chem. Biol. 3 (2007) 252.
[15] B. Gong, Acc. Chem. Res. 41 (2008) 1376.
[16] Z.-T. Li, J.-L. Hou, C. Li, Acc. Chem. Res. 41 (2008) 1343.
[17] C.E. Schafmeister, Z.Z. Brown, S. Gupta, Acc. Chem. Res. 41 (2008) 1387.
[18] D. Seebach, J. Gardiner, Acc. Chem. Res. 41 (2008) 1366.
[19] N.P. Chongsiriwatana, J.A. Patch, A.M. Czyzewski, M.T. Dohm, A. Ivankin, D. Gidalevitz, R.N. Zuckermann, A.E. Barron, Proc. Natl. Acad. Sci. U.S.A. 105 (2008) 2794.
[20] W.S. Horne, S.H. Gellman, Acc. Chem. Res. 41 (2008) 1399.
[21] E. Yashima, K. Maeda, Y. Furusho, Acc. Chem. Res. 41 (2008) 1166.
[22] J.S. Nowick, Acc. Chem. Res. 41 (2008) 1319.
[23] H.-J. Kim, Y.-B. Lim, M. Lee, J. Polym. Sci. A: Polym. Chem. 46 (2008) 1925.
[24] E. Yashima, K. Maeda, Macromolecules 41 (2008) 3.
[25] I. Saraogi, A.D. Hamilton, Chem. Soc. Rev. 38 (2009) 1726.
[26] J.C. Nelson, J.G. Saven, J.S. Moore, P.G. Wolynes, Science 277 (1997) 1793.
[27] H. Goto, J.M. Heemstra, D.J. Hill, J.S. Moore, Org. Lett. 6 (2004) 889.
[28] B. Adisa, D.A. Bruce, J. Phys. Chem. B 109 (2005) 19952.
[29] B. Adisa, D.A. Bruce, J. Phys. Chem. B 109 (2005) 7548.
[30] E.L. Elliott, C.R. Ray, S. Kraft, J.R. Atkins, J.S. Moore, J. Org. Chem. 71 (2006) 5282.
[31] R.F. Kelley, B. Rybtchinski, M.T. Stone, J.S. Moore, M.R. Wasielewski, J. Am. Chem. Soc. 129 (2007) 4114.
[32] L. Arnt, K. Nüsslein, G.N. Tew, J. Polym. Sci. A 42 (2004) 3860.
[33] Y. Ishitsuka, L. Arnt, J. Majewski, S. Frey, M. Ratajczek, K. Kjaer, G.N. Tew, K.Y.C. Lee, J. Am. Chem. Soc. 128 (2006) 13123.
[34] L. Yang, V.D. Gordon, A. Mishra, A. Som, K.R. Purdy, M.A. Davis, G.N. Tew, G.C.L. Wong, J. Am. Chem. Soc. 129 (2007) 12141.
[35] L. Yang, V.D. Gordon, D.R. Trinkle, N.W. Schmidt, M.A. Davis, C. DeVries, A. Som, J.E. Cronan Jr., G.N. Tew, G.C.L. Wong, Proc. Natl. Acad. Sci. U.S.A. 105 (2008) 20595.
[36] M. Inouye, M. Waki, H. Abe, J. Am. Chem. Soc. 126 (2004) 2022.
[37] K.-J. Chang, B.-N. Kang, M.-H. Lee, K.-S. Jeong, J. Am. Chem. Soc. 127 (2005) 12214.
[38] T.V. Jones, M.M. Slutsky, R. Laos, T.F.A. de Greef, G.N. Tew, J. Am. Chem. Soc. 127 (2005) 17235.
[39] N. Zhu, W. Hu, S. Han, Q. Wang, D. Zhao, Org. Lett. 10 (2008) 4283.
[40] H. Jiang, J.-M. Léger, I. Huc, J. Am. Chem. Soc. 125 (2003) 3448.
[41] C. Dolain, V. Maurizot, I. Huc, Angew. Chem. Int. Ed. 42 (2003) 2737.
[42] N. Delsuc, J.-M. Léger, S. Massip, I. Huc, Angew. Chem. Int. Ed. 46 (2007) 214.
[43] L. Yuan, H. Zeng, K. Yamato, A.R. Sanford, W. Feng, H.S. Atreya, D.K. Sukumaran, T. Szyperski, B. Gong, J. Am. Chem. Soc. 126 (2004) 16528.
[44] H. Goto, Y. Furusho, E. Yashima, J. Am. Chem. Soc. 129 (2007) 9168.
[45] H. Juwarker, J.M. Lenhardt, D.M. Pham, S.L. Craig, Angew. Chem. Int. Ed. 47 (2008) 3740.
[46] W. Vanormelingen, K. Van den Bergh, T. Verbiest, G. Koeckelberghs, Macromolecules 41 (2008) 5582.
[47] R.M. Meudtner, S. Hecht, Angew. Chem. Int. Ed. 47 (2008) 4926.
[48] W. Vanormelingen, A. Smeets, E. Franz, I. Asselberghs, K. Clays, T. Verbiest, G. Koeckebergh, Macromolecules 42 (2009) 4282.
[49] H. Goto, Y. Furusho, E. Yashima, Chem. Commun. (2009) 1650.
[50] H. Goto, Y. Furusho, K. Miwa, E. Yashima, J. Am. Chem. Soc. 131 (2009) 4710.
[51] C.-K. Liang, P.-S. Wang, M.-k. Leung, Tetrahedron 65 (2009) 1679.
[52] M. Miyasaka, M. Pink, S. Rajca, A. Rajca, Angew. Chem. Int. Ed. 48 (2009) 5954.
[53] G. Yuan, C. Zhu, Y. Liu, W. Xuan, Y. Cui, J. Am. Chem. Soc. 131 (2009) 10452.
[54] R. Méreau, F. Castet, E. Botek, B. Champagne, J. Phys. Chem. A 113 (2009) 6552.
[55] T. Ben, Y. Furusho, H. Goto, K. Miwa, E. Yashima, Org. Biol. Chem. 7 (2009) 2509.
[56] R. Kakuchi, S. Nagata, R. Sakai, I. Otsuka, H. Nakade, T. Satoh, T. Kakuchi, Chem. Eur. J. 14 (2008) 10259.
[57] V. Percec, M. Peterca, J.G. Rudick, E. Aqad, M.R. Imam, P.A. Heiney, Chem. Eur. J. 13 (2007) 9572.
[58] V. Percec, J.G. Rudick, M. Peterca, P.A. Heiney, J. Am. Chem. Soc. 130 (2008) 7503.
[59] Y. Zhao, A.D. Slepkov, C.O. Akoto, R. McDonald, F.A. Hegmann, R.R. Tywinski, Chem. Eur. J. 11 (2005) 321.
[60] C.A. Lewis, R.R. Tykwinski, Chem. Commun. (2006) 3625.
[61] J. Deng, W. Zhao, J. Wang, Z. Zhang, W. Yang, Macromol. Chem. Phys. 208 (2007) 218.
[62] Y. Liu, Y. Xin, F. Bai, S. Xu, S. Cao, Polym. Adv. Technol. 17 (2006) 199.
[63] G. Nannucci, L. Moroni, C. Gellini, R. Chelli, P.R. Salvi, V. Schettino, G. Delepiane, J. Phys. Chem. C 111 (2007) 17485.
[64] R.B. Prince, S.A. Barnes, J.S. Moore, J. Am. Chem. Soc. 122 (2000) 2758.
[65] L. Brunsveld, E.W. Meijer, R.B. Prince, J.S. Moore, J. Am. Chem. Soc. 123 (2001) 7978.
[66] T. Nishinaga, A. Tanatani, K. Oh, J.S. Moore, J. Am. Chem. Soc. 124 (2002) 5934.
[67] D. Zhao, J.S. Moore, J. Am. Chem. Soc. 124 (2002) 9996.
[68] K. Matsuda, M.T. Stone, J.S. Moore, J. Am. Chem. Soc. 124 (2002) 11836.
[69] Systems that utilize solvophobic interactions among non-adjacent repeat units to establish folded structures but are composed of non-arylene ethynylene backbones will not be covered in this review due to structural disparities. For examples of such foldamers, see Refs. [70–80].
[70] Y. Zhao, Z. Zhong, J. Am. Chem. Soc. 127 (2005) 17894.
[71] Y. Zhao, Z. Zhong, J. Am. Chem. Soc. 128 (2006) 9988.
[72] Y. Zhao, Z. Zhong, Org. Lett. 8 (2006) 4715.
[73] Y. Zhao, Z. Zhong, E.-H. Ryu, J. Am. Chem. Soc. 129 (2007) 218.
[74] Y. Zhao, Curr. Opin. Colloid Interface Sci. 12 (2007) 92.
[75] Z. Zhong, Y. Zhao, Org. Lett. 9 (2007) 2891.
[76] Z. Zhong, Y. Zhao, J. Org. Chem. 73 (2008) 5498.
[77] X. Pan, Y. Zhao, Org. Lett. 11 (2009) 69.
[78] Y. Zhao, J. Org. Chem. 74 (2009) 834.
[79] H. Cho, Z. Zhong, Y. Zhao, Tetrahedron 65 (2009) 7311.
[80] Y. Zhao, J. Org. Chem. 74 (2009) 7470.
[81] M.T. Stone, J.S. Moore, Org. Lett. 6 (2004) 469.
[82] K. Goto, J.S. Moore, Org. Lett. 7 (2005) 1683.
[83] H. Abe, N. Masuda, M. Waki, M. Inouye, J. Am. Chem. Soc. 127 (2005) 16189.
[84] M. Waki, H. Abe, M. Inouye, Chem. Eur. J. 12 (2006) 7839.
[85] M. Waki, H. Abe, M. Inouye, Angew. Chem. Int. Ed. 46 (2007) 3059.
[86] G.M. Whitesides, J.P. Mathias, C.T. Seto, Science 254 (1991) 1312.
[87] H. Abe, D. Murayama, F. Kayamori, M. Inouye, Macromolecules 41 (2008) 6903.
[88] H. Abe, H. Machiguchi, S. Matsumoto, M. Inouye, J. Org. Chem. 73 (2008) 4650.
[89] H. Abe, S. Takashima, T. Yamamoto, M. Inouye, Chem. Commun. (2009) 2121.
[90] R.B. Prince, T. Okada, J.S. Moore, Angew. Chem. Int. Ed. 38 (1999) 233.
[91] A. Orita, T. Nakano, D.L. An, K. Tanikawa, K. Wakamatsu, J. Otera, J. Am. Chem. Soc. 126 (2004) 10389.
[92] A. Orita, T. Nakano, T. Yokoyama, G. Babu, J. Otera, Chem. Lett. 33 (2004) 1298.
[93] T. Kawano, M. Nakanishi, T. Kato, I. Ueda, Chem. Lett. 34 (2005) 350.
[94] T. Kawano, T. Kato, C.-X. Du, I. Ueda, Tetrahedron Lett. 43 (2002) 6697.
[95] C. Li, Y. Guo, J. Lv, J. Xu, Y. Li, S. Wang, H. Liu, D. Zhu, J. Polym. Sci. A: Polym. Chem. 45 (2007) 1403.

[96] K.-J. Chang, D. Moon, M.S. Lah, K-S. Jeong, Angew. Chem. Int. Ed. 44 (2005) 7926.
[97] V.R. Naidu, M.C. Kim, J.-M. Suk, H.-J. Kim, M. Lee, E. Sim, K.-S. Jeong, Org. Lett. 10 (2008) 5373.
[98] U.-I. Kim, J.-M. Suk, V.R. Naidu, K.-S. Jeong, Chem. Eur. J. 14 (2008) 11406.
[99] J.M. Suk, K.-S. Jeong, J. Am. Chem. Soc. 130 (2008) 11868.
[100] D. Curiel, A. Cowley, P.D. Beer, Chem. Commun. (2005) 236.
[101] J.M. Heemstra, J.S. Moore, Org. Lett. 6 (2004) 659.
[102] J.M. Heemstra, J.S. Moore, Chem. Commun. (2004) 1480.
[103] J.M. Heemstra, J.S. Moore, J. Am. Chem. Soc. 126 (2004) 1648.
[104] J.M. Heemstra, J.S. Moore, J. Org. Chem. 69 (2004) 9234.
[105] R.A. Smaldone, J.S. Moore, J. Am. Chem. Soc. 129 (2007) 5444.
[106] R.A. Smaldone, J.S. Moore, Chem. Commun. (2008) 1011.
[107] S. Mecozzi, J. Rebek Jr., Chem. Eur. J. 4 (1998) 1016.
[108] O.-S. Lee, J.G. Saven, J. Phys. Chem. B 108 (2004) 11988.
[109] A. Khan, C. Kaiser, S. Hecht, Angew. Chem. Int. Ed. 45 (2006) 1878.
[110] A. Khan, S. Hecht, Chem. Eur. J. 12 (2006) 4764.
[111] J. Dokić, M. Gothe, J. Wirth, M.V. Peters, J. Schwarz, S. Hecht, P. Saalfrank, J. Phys. Chem. A 113 (2009) 6763.
[112] M.F. Perutz, M.G. Rossmann, A.F. Cullis, H. Muirhead, G. Will, A.C.T. North, Nature 185 (1960) 416.
[113] J.G. Ferry, Annu. Rev. Microbiol. 49 (1995) 305.
[114] M.T. Stone, J.S. Moore, J. Am. Chem. Soc. 127 (2005) 5928.
[115] J.W. Wackerly, J.S. Moore, Macromolecules 39 (2006) 7269.
[116] D. Zhao, J.S. Moore, Org. Biomol. Chem. 1 (2003) 3471.
[117] D. Zhao, J.S. Moore, J. Am. Chem. Soc. 125 (2003) 16294.
[118] P. Jonkheijm, P. van der Schoot, A.P.H.J. Schenning, E.W. Meijer, Science 313 (2006) 80.
[119] D. Zhao, K. Yue, Macromolecules 41 (2008) 4029.
[120] H.-J. Kim, W.-C. Zin, M. Lee, J. Am. Chem. Soc. 126 (2004) 7009.
[121] H.-J. Kim, E. Lee, M.G. Kim, M.-C. Kim, M. Lee, E. Sim, Chem. Eur. J. 14 (2008) 3883.
[122] H.-J. Kim, E. Lee, H.-s. Park, M. Lee, J. Am. Chem. Soc. 129 (2007) 10994.
[123] R.A. Blatchly, G.N. Tew, J. Org. Chem. 23 (2003) 8780.
[124] R.H. Grubbs, D. Kratz, Chem. Ber. 126 (1993) 149.
[125] T.V. Jones, R.A. Blatchly, G.N. Tew, Org. Lett. 5 (2003) 3297.
[126] S. Shotwell, P.M. Windscheif, M.D. Smith, U.H.F. Bunz, Org. Lett. 6 (2004) 4151.
[127] M.M. Slutsky, T.V. Jones, G.N. Tew, J. Org. Chem. 72 (2007) 342.
[128] T.V. Jones, M.M. Slutsky, G.N. Tew, New J. Chem. 32 (2008) 676.
[129] M.M. Slutsky, J.S. Phillip, G.N. Tew, New J. Chem. 32 (2008) 670.
[130] A. Khan, S. Hecht, J. Polym. Sci. A: Polym. Chem. 44 (2006) 1619.
[131] M.-X. Zhu, W. Lu, N. Zhu, C.-M. Che, Chem. Eur. J. 14 (2008) 9736.
[132] S. Toyota, M. Goichi, M. Kotani, M. Takezaki, Bull. Chem. Soc. Jpn. 78 (2005) 2214.
[133] S. Toyota, M. Goichi, M. Kotani, Angew. Chem. Int. Ed. 43 (2004) 2248.
[134] S. Toyota, S. Suzuki, M. Goichi, Chem. Eur. J. 12 (2006) 2482.
[135] S. Toyota, M. Kuga, A. Takatsu, M. Goichi, T. Iwanaga, Chem. Commun. (2008) 1323.
[136] R.B. Prince, J.G. Saven, P.G. Wolynes, J.S. Moore, J. Am. Chem. Soc. 121 (1999) 3114.
[137] M. Inoue, M. Teraguchi, T. Aoki, S. Hadano, T. Namikoshi, E. Marwanta, T. Kaneko, Synth. Met. 159 (2009) 854.
[138] R. Liu, M. Shiotsuki, T. Masuda, F. Sanda, Macromolecules 42 (2009) 6115.
[139] C. Tan, M.R. Pinto, M.E. Kose, I. Ghiviriga, K.S. Schanze, Adv. Mater. 16 (2004) 1208.
[140] X. Zhao, K.S. Schanze, Langmuir 22 (2006) 4856.
[141] A.E. Friedman, J.C. Chambron, J.P. Sauvage, N.J. Turro, J.K. Barton, J. Am. Chem. Soc. 112 (1990) 4960.
[142] Y.-Q. Huang, Q.-L. Fan, S.-B. Li, X.-M. Lu, F. Cheng, G.-W. Zhang, Y. Chen, L.-H. Wang, W. Huang, J. Polym. Sci. A: Polym. Chem. 44 (2006) 5424.
[143] M.A. Balbo Block, S. Hecht, Macromolecules 41 (2008) 3219.